CORROSION POTENTIALS OF LIGHTWEIGHT CONCRETE WRAPPED WITH FIBER REINFORCED POLYMERS (FRP)

by

ERIC GOUCHER

Presented to the Faculty of the Graduate School of

The University of Texas at Arlington in Partial Fulfillment

of the Requirements

for the Degree of

MASTER OF SCIENCE IN CIVIL ENGINEERING

THE UNIVERSITY OF TEXAS AT ARLINGTON

December 2013

Acknowledgements

I would like to thank Jack Sinclair of Trinity ES&C for donating the lightweight aggregates for use on this project.

I would like to thank Dr. Yazdani and Dr. Chao for all of their help they have given me during my time at UTA. Dr. Yazdani in particular has given me some very insightful ideas that have helped me to do this research. I would also like to thank Dr. Prabakar for his assistance.

I want to thank Istiaque Hasan and Joseph Williams for both of their help with me while doing this experiment. Istiaque's knowledge and Joseph's hard work made this research possible.

I want to thank everyone at UTA who I have been fortunate to become friends with over the past two years. It made the journey all the much more enjoyable.

Finally, thanks to my family: my parents and my brother, whose support has always enabled me to keep moving forward.

November 25, 2013

Abstract

CORROSION POTENTIALS OF LIGHTWEIGHT CONCRETE

WRAPPED WITH FIBER REINFORCED

POLYMERS (FRP)

Eric Goucher, M.S.

The University of Texas at Arlington, 2013

Supervising Professor: Nur Yazdani

The purpose of this research was to investigate the effects of Fiber Reinforced Polymer wraps on corrosion protection of lightweight concrete. Many studies have been undertaken for normal density concrete, but there are very few studies regarding lightweight concrete and externally bonded FRP wraps. This experiment involved the use of an accelerated corrosion test to determine the corrosion protection that FRP would afford lightweight concrete, while making a comparison with a similarly proportioned normalweight mix. 42 cylinders were subject to an constant 12 V power from a DC Power Supply while being immersed in a 5% NaCl for a period of 50 days. Samples were removed from the tank after failure and analyzed for chloride content and rebar mass loss. Current measurements were taken daily. The results indicated that both lightweight concrete and normalweight concrete greatly benefited from FRP wrapping in terms of increased time to failure and a reduction in rebar mass loss. Lightweight concrete generally performed better when wrapped with CFRP, whereas normalweight concrete generally performed better when wrapped with GFRP.

Table Of Contents

List Of Illustrations

List Of Tables

Chapter 1

Introduction

1.1 Background

America's infrastructure is currently outdated and insufficient in many areas. The 2013 edition of *ASCE's Report Card for America's Infrastructure* graded the overall state of America's infrastructure as a D+. According to this report, one in nine of America's bridges is rated as structurally deficient, and the average age of the bridges is 42 years. New construction is not always practical or economically efficient; it is necessary to devote research and resources to new materials and methods of repair to maximize the use of existing structures.

One area of study that has received great attention for repair is the use of Fiber Reinforced Polymers (FRP). These materials are very strong, light, and durable, making them a viable alternative to traditional methods of repair. They are primarily used to strengthen flexural, shear, and axial capacities of structural members, yet there have been many studies that have demonstrated their capabilities in upgrading the durability of structures, such as those exposed to corrosive elements. Examining the long term durability of FRP repaired structures is a major ongoing area of investigation. Most of these studies have examined the behavior of FRP with common materials such as normalweight concrete and steel, yet one area that has not received as much attention is structural lightweight concrete.

Lightweight concrete has been used for structural purposes for thousands of years, however it had limited capacity in structures until the rotary kiln process of producing lightweight aggregates arose in the early 20th century. Since then, lightweight concrete has become a viable alternative construction material to normal density concrete, often used in bridge elements such as decks, girders, and piers, in parking

garages, for office buildings, and for offshore platforms (ACI Committee 213). One prominent example is the Benicia-Martinez Bridge in California which uses high strength, sand-lightweight concrete in the entire superstructure, except at the pier caps (Murugesh, 2008). This bridge was the most cost effective of the options specified. Lightweight aggregate concrete, as its name suggests, contains lighter aggregates than normal density concrete, which can lead to advantages such as lesser dead load on structures which lowers the total weight of the structure. This can involve savings in both costs and weight, which can have advantages in reducing seismic forces. The National Cooperative Highway Research Program released report 733 (NCHRP, 2013) for high-performance/high-strength lightweight concrete for bridge girders and decks. This report suggested changes to parts of the AASHTO code in aspects such as creep and shrinkage losses, as well as equations to predict the modulus of elasticity and modulus of rupture. This report demonstrates the interest in using lightweight concrete as an alternative material to normal density concrete as the strength of lightweight concrete to reach comparable levels to normal weight concrete.

Despite these advantages, there are some drawbacks to the use of structural lightweight concrete. Many of these drawbacks are described in the construction of the Benicia-Martinez Bridge (Murugesh, 2008). Lightweight concrete in general has a lower modulus of elasticity and higher creep and shrinkage than normal density concrete. In seismic regions, high-performance concrete is often required to obtain the necessary strength and modulus of elasticity. For lightweight concrete this requires a very high amount of cement, which can make concrete brittle. Higher shrinkage can lead to cracking in concrete. Many of these issues can be mitigated through the use of supplementary cementitious materials and strong quality control measures, however instances where poor practices and inexperience with the use of new materials can lead

to cracking and problems where repair may be needed. This makes it necessary to research materials such as FRP to examine their behavior when used on lightweight concrete, in particular with regard to the aspect of enhanced durability when exposed to corrosive elements.

1.2 Research Objectives

The objective of this research is to examine the corrosion potentials of lightweight concrete with and without FRP. A lightweight concrete mix and a similarly proportioned normalweight concrete mix will be examined with and without FRP wraps. The samples therein will be exposed to an electric current and chloride solution. The corrosion activity will be monitored through impressed current flows, and reinforcement mass loss and chloride content will be examined. The effects of lightweight aggregate concrete reinforced with externally bonded FRP are not well known. ACI report 440.2 R-08 (ACI Committee 440, 2008) notes this, and recommends examining the these effects in its areas of future research. Since there is little information on this subject, this research is a preliminary investigation into the effects of FRP and lightweight concrete with respect to corrosion protection.

Chapter 2 Literature Review

2.1 Structural Lightweight-Aggregate Concrete

Structural lightweight concrete is defined as concrete which is made with lightweight aggregates conforming to ASTM C330, has a compressive strength in excess of 2500 psi at 28 days of age when tested in accordance with methods stated in ASTM C 330, and has an equilibrium weight not exceeding 115 lb/ft^3 as determined by ASTM C 567 (ACI Committee 211, 1998). This definition is not a specification but rather a guideline of sorts, as most projects containing lightweight concrete have densities in the range of 105-120 lb/ft^3. Densities in the range of 70-105 lb/ft^3 are not frequently used (ACI Committee 213, 2003).

The passages below will explain some of the history, properties, and applications of lightweight aggregates and lightweight concrete.

2.1.1 History of Structural Lightweight-Aggregate Concrete

Lightweight concrete has been used in structures for thousands of years. The Mediterranean region used natural lightweight aggregates from volcanic material to produce some early lightweight concrete structures. However, it wasn't until the 1900's and the invention of the rotary kiln process to manufacture lightweight aggregates that the material would become available for widespread commercial use. Ships and barges were some of the early adopters of reinforced lightweight concrete. The late 1940s brought about the use of lightweight concrete for home construction. In the 1950s multi story structures began using lightweight concrete, particularly in floor slabs, to reduce dead loads on the foundations. These different applications brought about an interest in studying the properties of lightweight concrete to produce concrete in applications that require high strength and performance. Research to produce high-strength lightweight concrete began in the 1980's, with the results produced in 1992. This research has

allowed lightweight concrete to be considered in areas that require high strength and durability, allowing it to be considered as a viable alternative to normalweight concrete in many applications (ACI Committee 213, 2003).

2.1.2 Structural Lightweight-Aggregate Properties

The rotary kiln process of manufacturing lightweight aggregates involves slowly heating a small particle of shale, clay, or slate in order to remove gases from the aggregate. These gases leave behind small cavities or pores that are retained after the aggregate has cooled. Thus, when lightweight aggregate is manufactured it develops a cellular structure, containing a system of pores in the range of 5 to 300 μm (ACI committee 213, 2003). This structure allows the lightweight aggregate to have much lower bulk and relative densities than its normalweight counterpart. Another effect of this pore system is that water absorption occurs directly into the aggregate itself, versus normalweight aggregate in which it occurs primarily on the surface. Lightweight aggregates can absorb from 5 to 25% of water by mass of the dry aggregate, whereas normalweight aggregates can absorb only around 2%.

The absorptive properties of lightweight aggregates create a condition known as internal curing when concrete is produced. Internal curing is a time-dependent process where moisture absorbed in the pores of lightweight concrete are slowly released into the cementitious portion of the concrete. This creates further hydration of the cement matrix in lightweight concrete over a long period of time, leading to long term strength improvements. (ACI Committee 213, 2003). The lengthened curing time increases the volume of cementitious products formed, which makes the pores in the cement paste closed or segmented (ACI Committee 213, 2003). Pores must be connected for harmful agents such as chlorides to have a path to the reinforcing bar. If these pores are segmented, there is no path for chlorides to travel, which reduces permeability.

2.1.3 Permeability of Lightweight Concrete

Lightweight aggregates are porous, therefore it would be a logical assumption that the permeability of lightweight concretes would be higher than for similarly proportioned normalweight concretes. However, ACI Report 213R (ACI Committee 213, 2003) notes several research studies that have shown that lightweight concrete has equal or lesser permeability than its normalweight counterpart .The primary reason for this is the superior interfacial transition zone between the aggregate and cement binder for lightweight concrete as opposed to the interface in normalweight concrete. Concrete permeability is generally a function of the quality of the cement matrix; lower quality pastes may develop micro cracks at the aggregate-cement matrix interface when stresses are applied that increase the susceptibility of the concrete to the intrusion of corrosive liquids. The improved aggregate-cement binder interface for lightweight concrete relies on various properties of the lightweight aggregate. The interface is a product of both mechanical interlocking between the lightweight aggregate and cement binder as well as a chemical interaction (Chandra and Bertsson, 2003). The chemical interaction involves a pozzolanic reaction between the lightweight aggregate and the cement binder. Aluminum and silicate products form on the surface of lightweight aggregates when they are fired at high temperatures during manufacturing. These products combine with calcium hydroxide to form new chemical products that help improve the interface. Another reason for the improved interface is the hygrol equilibrium that occurs in lightweight aggregates and the surrounding concrete paste (ACI Committee 213, 2003). In normal density concrete the aggregates contain very little absorption (around 2%). The surrounding cement matrix will contain much more water than the normal density aggregate, which will surround the particle instead of being absorbed into it and therefore will result in water bleeding. This bleeding can cause small

voids to occur. Lightweight aggregates due to their porous nature will contain water in them. This creates a balance between the water of the cement matrix and the water of the aggregate, which will in turn reduce the amount of bleeding which occurs and thus reduce the number of voids that occur. The similar elastic properties of the lightweight aggregate and the cement matrix also contributes to the interface zone (ACI Committee 213, 2003. The elastic properties in normal density aggregate are greater than the surrounding cement matrix. When stresses are applied to the concrete, this causes a differential stress in the cement matrix and the stiffer aggregate to occur, resulting in micro cracking. In lightweight concrete, the closer properties of the aggregate and cement matrix result in reduced or eliminated differential stresses. Also, as mentioned in the previous section, internal curing can extend the curing time of the cement products, which improves the cement paste and reduces the amount of connected pores that allow harmful substances to pass through to the reinforcing steel.

2.1.4 Types of Structural Lightweight Concrete

There are two different types of concrete that are made with lightweight aggregates: sand-lightweight concrete and all-lightweight concrete. Sand-lightweight concrete contains coarse lightweight aggregates and normalweight fine aggregates, generally sand. This is the most commonly used lightweight aggregate for structural purposes, due to the fact that it provides a weight reduction at a reduced cost compared to all-lightweight concrete .All-lightweight concrete contains lightweight aggregates in both the coarse and fine aggregate portions of the concrete mix. This type of concrete is generally lighter than sand-lightweight concrete, but is more expensive. Due to the porous nature of the lightweight aggregates, all-lightweight concrete is also much more porous than sand-lightweight concrete, which can lead to greater chloride penetration.

2.1.5 Structural Lightweight Concrete Applications

As mentioned in the introduction, there have been several applications of lightweight concrete since the commercialized production of lightweight aggregates using the rotary kiln process came about. Parking structures that have 50-to-63 foot spans are often constructed with double-tee members with lightweight concrete having densities around 115 lb/ft^3 (Holm and Bremner, 2000). A five-story parking garage in North Carolina used lightweight concrete columns with 9000 psi strength in order to precast and transport the columns in one piece. These columns weighed 125 lbs/ft instead of 155 for a comparable normalweight concrete, with the longest column being 73 feet high, resulting in significant weight reductions for transport (Mackie, 1985). Large submerged pipe structures have been constructed with lightweight concrete (Holm 1980). Floating bridge pontoons will often use high performance lightweight concrete for their reduced density. When lightweight concrete is submerged, it further magnifies the reduction in density that it already has over normalweight reinforced concrete. A reduction of 25% will be expended to 50% when submerged (ACI Committee 213, 2003). For this reason, many offshore structures will use lightweight concrete to take advantage of these properties.

Several bridges have incorporated lightweight concrete in either new construction or rehabilitation, with the greatest utilization by far being in the decks to take advantage of the reduction in density over a large area. Many bridges use lightweight decks to reduce loads on the foundations, or to widen bridge decks for rehabilitated bridges. For equivalent density normalweight and lightweight decks, the lightweight deck can be built with a thicker depth, so the concrete cover to rebar can be increased (ACI Committee 213, 2003). There are many advantages to using lightweight concrete in bridge decks,

and oftentimes their advantages in weight reductions have offset the increased costs that lightweight aggregates have over normalweight concrete.

With greater strengths being realized by lightweight concretes, bridge girders have also been able to take advantage of the use of lightweight concrete. The Parrotts Ferry Bridge in California used precast, post-tensioned single cell box girders in the bridge (Mackie, 1985). This bridge was built in the 1970s and at the time was the longest span built in the US by the segmental cantilever construction method, at 640 feet. The Benicia-Martinez Bridge mentioned in the introduction contains lightweight concrete throughout the superstructure. This bridge is another segmental bridge with span lengths from 525 to 663 feet, for a total 1.4 mile long crossing (Murugesh 2008). In regions of seismic activity lightweight concrete is particularly being utilized due to the reduction in dead load.

The *Guide for Structural Lightweight-Aggregate Concrete* (ACI Committee 213, 2003) has also mentioned that lightweight concrete has been used for bridge piers, but specific instances of that have been very difficult to find in the literature. It is certainly much less common to use lightweight concrete for the bridge substructure as it is for the superstructure.

2.1.6 Structural Lightweight Concrete Use in Texas

Texas has incorporated lightweight concrete in parking garages and multi-story buildings similar to other states, but its use of lightweight concrete in bridges is fairly limited. Most lightweight concrete has been restricted to bridge decks. Heffington (2000) researched repeatable high strength lightweight concrete mixes for prestressed bridge girders using locally available expanded shale and clay aggregates from Texas Industries (TxI). Mixes for 6000 psi and 8000 psi sand-lightweight concrete were investigated. Two 40-foot pretensioned bridge girders and three 40-foot pretensioned bridge girders were

fabricated from the 6000 psi and 8000 psi mixes, respectively. Strength, creep, shrinkage, and workability tests were carried out. The results of the research indicated the 6000 psi mix performed very well and could be respecified as a 7000 psi mix, whereas the 8000 psi mix did not perform adequately and was changed to a 7500 psi mix. The research recommended that lightweight deck panels be considered as an alternative to normalweight deck panels, and that lightweight girders be used as an alternative to normalweight girders if necessary. In February 2002 TxDoT stated it would not implement deck panels due to questions regarding economic feasibility and tensile stress limits (Heffington et al., 2001). Information on the current status of high performance precast lightweight concrete use in Texas is not readily available.

2.2 Fiber-Reinforced Polymers (FRP)

Fiber Reinforced Polymers (FRP) are composite materials, consisting of fibers embedded in a resin matrix. The passages below examine some of the history of FRP composites, their properties, and their uses in the construction industry.

2.2.1 History of FRP Composites

The first known FRP product was a boat hull manufactured in the mid-1930s using fiberglass fabric and polyester resin (ACI Committee 440R, 2007). Since the 1940s the defense industry has been using FRP composites for naval and aerospace uses. These materials were later made available to the public sector and found particular use in the manufacturing industries where chemicals are largely involved.

The construction industry has used FRP composites since the mid-1950s, when the ability to reinforce concrete structures with FRP was first demonstrated (ACI Committee 440R, 2007). In the 1980s the materials became more profound within the construction industry as FRP reinforcing bars were developed for concrete required for special performance. Bridges in particular began using FRP in their design more frequently, especially in Europe and Asia. In 1986, the first highway bridge that used composite reinforcing tendons was constructed in Germany. China constructed the world's first all-composite bridge deck, and the first all-composite pedestrian bridge was installed in Aberfeldy, Scotland, in 1992. In the U.S. the first FRP-reinforced bridge deck was built in 1996 in McKinleyville, West Virginia, and the first all-composite vehicular bridge deck in Russell Kansas followed shortly thereafter.

Since the 1990s the FRP market has considerably grown. According to the *Composite News International* the composites industry in North America was estimated at $9 billion (ACI Committee 440R, 2007).

2.2.2 FRP Composite Properties

As noted earlier, FRP composites consist of strong fibers embedded in a resin matrix. The role of the fibers in the composites is to provide strength/load-bearing capacity and stiffness, whereas the role of the polymer matrix is to keep the fibers in place, allow stress transfer between fibers, and provide protection from the environment.

FRP composites are anisotropic materials. They are typically strongest along the length of the fiber itself, and weakest along the transverse direction of the fiber. This is different from isotropic materials such as steel where their mechanical properties are the same regardless of orientation. They also differ from steel by exhibiting elastic behavior until failure. When FRP fails it is generally a very brittle form of failure, whereas steel will go through a plastic state of failure and yield before it fails.

2.2.2.1 FRP Fibers

As a composite material, FRP properties are a function of both the fiber and polymer matrix. The selection of materials that comprise the FRP composite must be made with an understanding of what the material will be used for. There are three common fiber types used for FRP systems: glass, carbon, and aramid.

Glass fibers are the most commonly used type, due to the fact that they are less expensive than carbon fibers while still providing high strength properties. Commercial glass fibers are available as electrical grade (E-glass), which is the most commonly used general-purpose FRP fiber; high strength (S-2) glass, improved acid resistance (ECR glass), and alkali resistant (AR glass). Glass is denser than carbon and aramid fiber types, and is a very good electrical and thermal insulator (ACI Committee 440R, 2007).

Carbon fibers are about five to ten times more expensive than glass fibers, but they have twice the strength and four times the stiffness of glass fibers (ACI Committee

440R, 2007). They are also very durable. Since they are very expensive, they are most suitable in situations such as bridge repair where high strength may be needed.

Aramid fibers are organic fibers. They have very low density, high strength, and provide impact resistance. They degrade under exposure to ultraviolet radiation, and they absorb moisture up to 10% of their fiber weight (Gangarao et. al., 2006). As such, they are not suited as well as carbon fibers for applications in harsh environments.

ACI 440R-07 gives typical properties of the different types of fibers. E-glass has a tensile strength of 500 ksi and a tensile modulus of 10,500 ksi. Carbon fibers range from 275 to 820 ksi in tensile strength and 32,000 to 110,000 ksi in tensile modulus. Aramid kevlar has a tensile strength of 525 ksi and a tensile modulus of 19, 000 ksi (ACI Committee 440R, 2007). For comparison purposes, a common reinforcing steel bar has a tensile strength of 60 ksi, whereas a steel prestressing strand has a tensile strength of 270 ksi. While the FRP will not be as strong as the fiber itself since it is a composite material, the resulting composite is extremely strong, thus showing its attractiveness as an alternative to other repair materials for structural member strengthening.

2.2.2.2 Resin matrix

Resins can either be thermoset or thermoplastic. Thermoplastic resins become soft when heated, and can then be shaped or formed while in that state. Once they cool they become rigid. Thermoset resins, on the other hand, are initially liquids or low melting point solids that harden once they have been heated (ACI Committee 440R, 2007).

FRPs generally contain thermoset resins. They include epoxy, esters, polyesters, vinyl esters, and phenolic materials, with polyester, epoxy and vinyl ester being used frequently. Polyester resins are inexpensive, but have problems adhering to many surfaces and can emit harmful air emissions. Epoxy resins have excellent

mechanical properties, and also provide resistance to several environmental effects such as corrosion and elevated temperatures. They provide a strong adhesive to a substrate, making it very useful for concrete repair where the material must be bonded to the concrete surface. Vinyl ester is a combination of polyester and epoxy, so it has characteristics of both, although it emits air pollutants similar to polyester resins (Park et. al, 2002).

2.2.3 Externally Bonded FRPs

FRPs can be used in both new construction or as a repair material. New construction typically involves reinforcing bars made of FRP used in place of normal steel reinforcement, such as in bridge decks. This is known as internal FRP reinforcement. Externally bonded FRPs are generally used as repair materials, and bond to the concrete surface or substrate.

There are a number of different externally bonded FRP repair systems. One is using the FRP as a jacket, essentially creating a form around a structural member and filling it with concrete or mortar. This method usually fails due to an installation or material deficiency, such as delamination of either the FRP or the filler material from the substrate (Wootton et. al., 2003). Another repair system, and the most common type, is applying the FRP as a laminate or sheet, and bonding it directly to the surface of the structural member using a wet layup system. This will be detailed in the next section. Near surface mounting is another technique that involves placing FRP bars or strips into small grooves or slots cut into the concrete cover. This method is typically easier to apply than the laminate method. A newer technique is known as mechanically fastened FRP, in which strips of FRP material are bolted into the concrete material itself. This method is the easiest to apply and can be done with tools on the jobsite, but it can cause stresses at the points where the bolts are applied. The research pertaining to this thesis

involves FRP sheets, otherwise known as "FRP wraps", so the rest of the information contained in this document will apply to this type of FRP system.

2.2.4 Application methods of FRP

FRP sheets can be applied to a structure through three methods. The first method is known as wet lay-up. This involves taking dry fibers and thoroughly saturating them on site, using tools such as trowels, and then directly applying the composite to the structure. The resin may also be applied to the structure first to ensure a good bond. In this method, the composite will cure on site. The performance of wet lay-up systems depends on the quality of the bond performed on site.

Another method is the use of prepreg systems. In this system the fiber sheets are saturated off site at a manufacturing plant, then applied in the same way as the wet lay-up system. They will also cure on site after application. These systems are generally of better quality than FRP applied via the wet lay-up method (Park et al, 2002).

The third method involves precured systems. In this case, the resin is applied off site similar to the prepreg system and cured as well. However, since they are already cured, there can be problems achieving a strong bond to the surface (Park et al., 2002).

For any of these methods, it is imperative to achieve good bond. The concrete surface must be cleaned and free of any dust or small particles that can interfere in the bonding process. The concrete is also usually roughened to expose the aggregate in order to help bonding.

2.2.5 Uses of FRP in the construction industry

FRPs are typically used to repair, rehabilitate and strengthen damaged and deficient structures. They have been used to strengthen concrete beams in flexure and shear, slabs in flexure, and columns in compression, flexure, and shear (ACI Committee 440R, 2007).

Where FRP is applied on the member depends on the intent of repair. For example, beams strengthened in flexure will have FRP sheets applied on the tension side. For shear strengthening, FRP may be applied to both sides of the member, three sides of the member (U-wrapping), or on all four sides. Wrapping on all four sides will lead to the greatest increase in shear strength (Park, 2002). Columns that are completely wrapped with FRP can achieve great increases in capacity due to the effects of confinement that FRP can provide.

There has been considerable research regarding the strengthening effects that FRP materials provide. What is less clear is the long-term durability effects of structures reinforced with FRP. As the use of FRP for structural repair is relatively new, long term data is not yet available on these systems, so universal acceptance of FRPs is still ongoing . Since FRPs are used for bridges, parking garages, and other locations where the environment is present, there is interest for continuing research on the effects of moisture, ultraviolet radiation, alkaline solutions, extreme temperatures, and other potentially harmful factors on FRP systems. Corrosion in particular is an area where FRP materials have proved beneficial in mitigating its effects. Investigations of the use of FRP to protect against corrosion will be examined in greater detail in the next section.

2.3 Corrosion of Steel Embedded in Concrete

2.3.1 Corrosion Mechanics

The corrosion of metal is an electrochemical process that involves the transfer of electrons between an anodic site and a cathodic site. The anode produces electrons while the cathode consumes them. Two half-cell reactions much take place for an electrochemical reaction to occur. For reinforced steel in concrete, this includes the anodic reaction in the oxidation of iron, as well as the cathodic reaction in the formation of hydroxyl ions, OH-. The following half-cell reactions occur for steel embedded in concrete (ACI Committee 222R, 2001):

Anodic Reactions:

$$Fe \rightarrow Fe^{++} + 2e^{-} \quad (2.3.1)$$

$$2Fe^{++} + 4OH^{-} \rightarrow 2Fe(OH)_2 \quad (2.3.2)$$

$$2Fe(OH)_2 + 1/2O_2 \rightarrow 2FeOOH + H_2O \quad (2.3.3)$$

$$Fe + OH^{-} + H_2O \rightarrow HFeO_2^{-} + H_2 \quad (2.3.4)$$

Cathodic Reactions:

$$2H_2O + O_2 + 4e^{-} \rightarrow 4\ (OH)^{-} \quad (2.3.5)$$

$$2H^{+} + 2e^{-} \rightarrow H_2 \quad (2.3.6)$$

Concrete naturally contains a high alkalinity environment with a pH of approximately 13. This high alkalinity environment allows the generation of a protective passive film around the reinforcement that occurs from the iron oxide reactions that occur during the hydration of concrete. This passive film forms a barrier against corrosion. Corrosion initiates by the breakdown of this barrier. The two processes that can remove this barrier are attack of ions such as chlorides, or the reduction of pH in the system through carbonation.

The removal of the passive film with chloride ions is the most common cause of corrosion in reinforced concrete. Structures in marine environments are subject to seawater salts that contain chloride ions. Deicing salts that are used on roads can also subject the concrete to chlorides. These chloride ions breakdown the passive film and react with the ferrous ions from the rebar; this creates an iron hydroxide compound once it reaches the high pH of the concrete. This breakdown of the passive film is generally locally concentrated, becoming anodic which attracts more chloride ions from the cathode. The iron hydroxides react to oxygen to create rust. These hydroxides occupy a volume greater than the material that they come from, as much as two to six times, so which places internal stresses from the rebar to the surrounding concrete, leading to cracking (ACI Committee 222R, 2001). Therefore, in order for corrosion to occur due to chloride attack, it is necessary to have moisture to provide the chloride ions to remove the passive film, and oxygen to react with the iron hydroxides.

Carbonation is the other process which leads to corrosion. With carbonation, the passive film of the concrete is reduced due to the reaction of the alkaline in cement and carbon dioxide in the atmosphere. Carbonation is generally not very common, however areas that contain high levels of CO_2 in the atmosphere, such as industrial zones, are at increased risk of this happening. Carbonation and chloride ions can work together to destroy the passive film surrounding the rebar.

Depending on the location of the anode and cathode, a system where the electrochemical process occurs may be deemed as a macrocell or microcell. For a macrocell the location of the anode and cathode are far away from each other. Daily (2003) provides an example of a macrocell through the application of de-icing salts on a bridge deck. If the deck has an upper mat of steel and lower mat of steel, the upper mat of steel will naturally have a greater concentration of chloride ions. Therefore, the

passive film of the upper mat will be removed first, causing the upper mat to become an anode and the lower mat to become a cathode.

2.3.2 Properties of concrete that affect corrosion

There are several properties of concrete that can influence the corrosion of reinforcing steel. A properly designed mix can enhance the corrosion resistance of the reinforcing steel. The cement paste of concrete contains several small pores that can connect together to lead a path for water and gases to flow to the reinforcing steel. A low water/cement (w/cm) ratio can reduce the sizes of these pores to reduce the amount of flow that can occur. Cement contains C_3A, tricalcium aluminate, which can react with chloride ions, thereby reducing the number of chloride ions that can reach the reinforcing steel. High alkalinity cement can increase the alkalinity of the concrete which helps produce the passive barrier around the steel, although too much can lead to a negative alkali-aggregate reaction. Different type of aggregates have different properties and sizes, which can affect the interface between the cement paste and the aggregate and the pores that can occur in the paste. Chemical and mineral admixtures are often used in concrete. Air-entraining admixtures and water-reducing admixtures both have the ability to reduce the water needed in a concrete mix, which lowers the w/cm ratio. Accelerating admixtures can reduce concrete setting times and improve strength, however many accelerators use calcium chloride, which can lead to chloride ions in the concrete mix that attack the passive film. Corrosion inhibiting admixtures are often used to delay and reduce the corrosion of reinforcing steel. Mineral admixtures such as fly ash have very small particles which can fill the pores in the cement paste, thus the number of pores that the chloride ions can pass through is reduced. These are often very effective in corrosion protection and are used in practically all environments that are expected to be subject to corrosion.

Along with the actual concrete itself, there are other factors that can influence corrosion. This includes concrete clear cover, where an increased distance from the concrete surface leads to longer paths for liquids and gases to flow to get to the rebar. Other corrosion prevention measures such as epoxies are often used on the rebar themselves. FRP has been found to have excellent corrosion resisting properties; these will be detailed later in this section.

2.3.3 Corrosion studies of Structural Lightweight Concrete

The porous structure and engineering properties of lightweight aggregates attribute to the creation of concrete that contains several advantages, as well as disadvantages, from normalweight concrete. This section will concentrate on studies related to the properties of lightweight concrete that affect corrosion. Most studies involve the use of admixtures such as silica fume and fly ash to provide corrosion resistance.

Zhang and Gjorv (1991) studied the permeability of high-strength lightweight concrete. They created 9 lightweight mixes with variables including the amount of cement and silica, water cement ratio, mix proportions, type of lightweight aggregate, and amount of natural sand used. These samples were then tested for water penetration, chloride permeability, and electrical conductivity. The results indicated that the permeability of the lightweight concrete seemed to be more dependent on the porosity of the mortar matrix rather than lightweight aggregate porosity, and an optimum amount of cement was observed in which too much would increase the permeability. They also noted that accelerated testing of chloride penetration was more valuable than electrical conductivity in determining permeability.

The Carolina Stalite Company examined the difference in the rapid chloride permeability of similarly proportioned lightweight and normalweight concretes (Wall and

Freeman, 2003). Four lightweight aggregate mixes utilizing expanded slate aggregate were utilized along with four comparable normalweight mixes. The mixes varied using no mineral admixtures, fly ash, silica fume, and fly ash and silica fume together. Concrete cylinders were produced from each mix , wet cured for 28 days and air-dried until they were 150 days old. The chloride permeability of all the cylinders was determined using ASTM 1202. The results indicated that for no admixtures, the lightweight and normalweight concrete performed nearly identically, however for the mixes with admixtures involved, the lightweight concrete performed greater than the corresponding normalweight mixture. Silica fume in particular showed vast improvement in lightweight concrete over normalweight concrete, with an average of 985 coulombs lower in chloride permeability. The authors attribute this to the high quality transition zone in the cement paste matrix as well as the extended curing time from internal curing.

Liu et al. (2010) evaluated the development of lightweight concrete with high resistance to water and chloride-ion penetration. The influence of different coarse and fine lightweight aggregates on water absorption, water permeability, and resistance to chloride-ion penetration were examined. Another objective was to determine whether the lightweight aggregates or the surrounding paste matrix were the dominant force in porosity of concrete. Seven concrete mixes were evaluated that varied the coarse and fine aggregates, as well as the quality of the paste matrix in order to determine whether the porosity of the aggregates or porosity of the paste matrix controlled for transport of water and chlorides throughout the concrete. Both sand lightweight concrete and all lightweight concrete were examined. The results indicated that the incorporation of LWA increased water sorptivity and permeability slightly in comparison with normalweight aggregates. For sand-lightweight concrete, more porous lightweight aggregate tended to reduce resistance to chloride-ion penetration. Sand-lightweight aggregate tended to

have greater resistance than all-lightweight due to the increased porosity from the inclusion of the porous fine lightweight aggregate. Finally, the water accessible porosity tended to have a greater effect on the transport properties of the concrete than the overall concrete porosity, which was measured by concrete unit weight.

These research experiments represent some of the aspects that make lightweight concrete particularly attractive in corrosive environments. New construction with high strength lightweight aggregate concrete enhanced with admixtures can exhibit high corrosion resistance. For existing deteriorated structures and structures in need of repair, the use of systems such as FRP can be used to provide corrosion resistance. These studies are detailed in the next section.

2.3.4 Corrosion studies of concrete treated with FRP strengthening systems

The first application of FRP for corrosion repair occurred in a bridge in Japan in 1977 (Sen 2003). The bridge, in service for 20 years prior to that point, had developed severe cracks due to corrosion. In the worst conditioned the GFRP was applied in two layers to the webs, and a steel plate bonded to the bottom flange. In all other beams, the GFRP was applied in one layer to the entire surface. In 1990 the bridge was replaced so the opportunity to determine the effectiveness of the FRP treatment presented itself. It was found that the FRP was capable of reducing the ingress of further chloride ions, however it did not affect the corrosion that was already present.. In another investigation at the University of Texas at Austin, Berver et. al. (2001) tested fourteen reinforced concrete specimens subject to wet/dry cycles with 3.5% saline water. Ten specimens were wrapped with GFRP, while four were used as control. Some specimens were cracked beforehand and then repaired with the GFRP wrap, and half of the specimens had chlorides 1.5% by weight of cement artificially input in the concrete mix. They found

that the wrap did not prevent corrosion activity in specimens that already had corrosion present, but did provide a barrier to further chloride ingress.

Suk et. al. (2007) conducted a long term study investigating 1/3 scale prestressed piles, wrapped with CFRP and GFRP, that were subjected to simulated tidal cycles for nearly 3 years. These specimens were 6 in by 6 in by 5 feet, prestressed with four 5/16 in, low-relaxation strands. Twenty wrapped specimens and four control specimens were placed in a tank and exposed to simulated tidal cycles of 3.5% salt water. Half-cell and linear polarization measurements were taken for current measurements and corrosion rate measurements. After exposure, bond tests, crack mapping, and gravimetric testing for metal loss were undertaken. They found that wrapped specimens had significantly lower metal loss than unwrapped. They noted that GFRP and CFRP specimens performed similarly. Another finding that other researchers have noted is that more layers used are not as effective; rather, two layers is shown to be the optimum amount.

Due to the slow nature of corrosion, it is often necessary to use accelerated corrosion tests. Since the current thesis uses an accelerated corrosion test, several research studies that incorporate this test type will be explored below.

2.3.4.1 Accelerated Corrosion Tests Using Impressed Current

Since natural corrosion can take a long period of time to occur, accelerated corrosion tests have been used in research to produce results in a reasonable amount of time. There are several different methods to induce corrosion in reinforced concrete specimens. These include salt spray, chloride diffusion, alternate drying and wetting in salt water, and impressing anodic current. Salt spray involves spraying a dissolved sodium chloride mist onto specimens inside an enclosed chamber. Chloride diffusion is a process in which chloride ions are artificially placed in the concrete during mixing, so they

are always present in that concrete. Alternate wet-dry cycles can simulate splash zones and are often used in studies. However, the quickest method is using impressed current (Gadve et. al, 2008). This involves placing concrete into a salt solution and passing a direct current with a power supply through the rebar. A nobler metal to rebar such as stainless steel is used as a cathode and connected to the other terminal of the power supply.

Detwiler et. al. (1991) looked at the effects that curing concrete at different temperatures had on resistance to chloride intrusion. Three different mixes with water cement ratios of 0.40, 0.50, and 0.58 were utilized with curing temperatures of 5, 20, and 50 C. The mixes were reproduced three times in order to cure at the three listed temperatures, therefore there were nine mixes in total. A chloride diffusion test was performed on one 4 in by 8 in cylinder, and a chloride penetration test was done on three 4 in by 11 in cylinders. The penetration test was an accelerated corrosion test using induced current. The lollipop specimens were placed in a tank and connected to a 12 V power source. The rebars of the specimens acted as anodes, whereas steel plate electrodes were used as cathodes so that corrosion could begin occurring. A data logger was used to collect current measurements in order to ensure everything was working properly. The results of these tests found that concrete cured at higher temperatures were less durable than at lower temperatures. Also, lower w/c ratios were influenced by curing temperatures more intensely than higher ratios. They also noted that the effects of poor consolidation and bleeding had greater impact than w/c ratios and curing temperatures.

Spainhour et. al. et. al. (2002) investigated the use of CFRP wraps to reduce the intrusion of chloride ions into steel reinforced concrete , and as a result would provide protection against the onset of these ions. The theory behind the use of FRP wrapping

directly to a surface , versus a system such as FRP jacketing, is that the wraps would bond better to the surface and provide a confinement effect to the concrete, which would help prevent concrete from spalling due to the volume expansion of the concrete from corrosive products forming on the reinforcing bars. This investigation comprised two different studies. In the first part, large reinforced column samples were wrapped with CFRP and long-term durability studies with heated wet/dry cycles for up to 2.5 years were conducted. These studies included half-cell measurements, reinforcing bar mass loss, and chloride content investigations. The effect of wrapping initially before applying corrosion and wrapping after a one year period of time had elapsed were investigated. In the second part of the experiment, accelerated short term corrosion studies similar to the one by Detwiler were carried out. Forty-two 2 in by 4 in cylinders were subjected to accelerated corrosion testing through impressed current for approximately two months. Similar to the Detwiler experiment, the cylinders were submerged in a tank with a 5% by weight NaCl solution. The samples were wired so that the rebars were anodic and steel plates were used as cathodes, with a 12 volt charge passing through the system from a power supply. The test variables included wrap orientation (radially, axially, or at a 45 degree angle), two different types of epoxy, the use of epoxy only, and the use of one or multiple layers (up to 3) of CFRP. The setup for the short term studies is detailed below. This experiment is the basis for the current investigation in this thesis.

Figure 2-1 Accelerated Corrosion Experiment (Spainhour 2002)

The results for the first experiment indicated that for both initial wrapped specimens and specimens wrapped in one year it took longer to reach a 90% probability of corrosion, chloride content was reduced, and less rebar mass loss occurred. After one year the chloride contents for wrapped columns were 2 to 8.5 times less than the unwrapped columns. The average rebar mass loss for unwrapped columns was 5.8% per year, versus 4.8% for columns wrapped at the beginning of the experiment. Columns wrapped after one year had rebar mass loss of 7.57 percent after two years, which was 50% less than the unwrapped samples and only 18% higher than samples that were wrapped at the beginning of the experiment. For the second experiment, it was discovered that the type of epoxy had a large influence on the corrosion resistance, whereas the use of epoxy alone was not as effective as confinement with FRP wraps. Two layers of FRP were shown to have greater effect in corrosion resistance than one

layer, but three layers were not necessarily any more effective than two layers. It was also shown in the results that samples with CFRP wrapping performed better than samples with epoxy alone. In addition, FRP wrapped radially showed the best results in terms of corrosion resistance due to the effects of confinement that the wraps provided.

Gadve et.al. (2009) investigated the use of FRP wraps in providing active and passive protection to steel reinforcement in concrete that had already been damaged by corrosion. Concrete cylinders with dimensions of 4 in by 9 in embedded steel reinforcement were subjected to accelerated corrosion to initiate cracking, then wrapped with either GFRP or CFRP, then subjected to further accelerated corrosion. The initial accelerated corrosion involved placing the specimens in a 3.5% solution and impressed with a constant 100mA direct current for up to 8 days. After cracking, the cylinders were wrapped and the experiment continued for a total duration of 24 days. The results showed wrapping dramatically decreased the rate of corrosion and loss of mass in the steel reinforcing bars, while increases were observed in pullout strength and corrosion current. Cell voltages of wrapped specimens were seen to have increased by approximately 300%. Also of note was that GFRP appeared to impede corrosion more than carbon. A possible explanation is that glass has higher electrical resistance than carbon. Another explanation is that GFRP sheets are typically thicker than CFRP sheets.

Maaddawy et. al. (2006) subjected thirty five 4 in by 8 in concrete cylinders to accelerated corrosion, while varying the level of applied potential, presence of FRP wraps, and bar diameter. Normal strength concrete of approximately 5000 psi compressive strength was used, with 3% NaCl by weight of cement added to the mixture. SikaWrap Hex103C Fibers and Sikadur Hex 300 resin were used for CFRP and epoxy. The voltage applied was low using 15 V or high using 60 V, with bars ranging from No. 10 to No. 20. The results indicated that under the same applied fixed potential, CFRP wraps

reduced current and mass loss, with mass loss on average 36% lower than unwrapped specimens. For the same applied potential fixed potential and cathodic surface area, reducing bar diameter increased current density level. Raising the potential level four times raised the current level the same amount, however, the steel mass loss increase was only around 37% and 57% for unwrapped and wrapped specimens. CFRP delayed the time from corrosion initiation to initial cracking about 20 times longer than that for unwrapped specimens. The theoretical mass loss by Faraday's Law was in good agreement with actual corrosion up to 10% mass loss, but were lower than that predicted by Faraday's Law for higher mass losses.

Masoud and Soudki (2006) looked at corrosion activity of FRP wrapped beams. Ten beams of dimensions 6 in by 12 in by 10.5 feet were cast. One beam was used as a reference, three corroded and not repaired, and the other six corroded and repaired with FRP sheets, followed by further accelerated corrosion for all of the beams. To accelerate the corrosion, 2.15% NaCL by weight was used in the flexural zone of the beams and an impressed current was applied. Both CFRP and GFRP sheets were used for this test, which lasted up to 200 days. Two repair schemes were used; one included wrapping the beam cross section with GFRP in a U-wrap scheme, whereas the other added CFRP for flexural strengthening along with the U-wrapped GFRP. Half-cell measurements and mass loss of the bars were monitored. They concluded that the mass loss of the bars were 16% for the repaired specimens versus the control. In addition, the U-wrapped GFRP was the main deterrent for the corrosion, whereas the flexural strengthening for the CFRP had no significant effects on corrosion activity.

Several research experiments regarding corrosion of concrete wrapped with FRP have had several findings in common. FRP wraps can be used to provide a barrier for against chloride penetration, however chlorides that are already in the concrete will

continue to corrode the reinforcing steel inside. Both CFRP and GFRP wraps have been investigated in regards to corrosion resistance, and both have been found to provide good protection against corrosion. The use of multiple layers is largely ineffective against further corrosion protection beyond the use of two layers. The choice of epoxy is very important when determining which FRP system is used. Finally, it appears that wrapping schemes that incorporate some kind of confinement, such as complete wrapping for columns or U-wrapping for beams, are more effective at controlling corrosion than wrapping schemes that involve only a portion of the structure, such as flexural reinforcement schemes for a beam.

Although the effects of corrosion have been investigated in several research papers in regard to normalweight concrete, very little information if any has been presented on lightweight concrete that utilizes FRP wraps. Since lightweight concrete has been used in structures with exposure to corrosive environments since the mid-1900s, and higher strengths of lightweight concrete is being realized for structures built today, there is benefit to understanding the properties of FRP wrapped lightweight concrete. The research below will attempt to investigate the behavior of these systems together with regards to corrosion.

Chapter 3

Procedure

3.1 Background on the experiment

The purpose of the experiment was to examine the effects of FRP wrapped lightweight concrete in regards to corrosion protection. There have been several corrosion experiments on normalweight concrete with FRP wraps. Normalweight concrete has a density in the range of 140-155 lb/ft^3 and is made with ordinary aggregates such as sand, gravel, crushed stone, limestone, etc. As detailed in the literature review, lightweight concrete used for structural purposes has a density in the range of 105-120 lb/ft^3, and is made of manufactured clay, shale, or slate. For the purposes of the rest of this thesis, lightweight concrete will mean sand-lightweight concrete, which is what is typically used for structural applications. All-lightweight concrete was not considered for this experiment, and so the term lightweight concrete will only apply to sand-lightweight concrete in this paper.

Since natural corrosion is a very slow process, an accelerated corrosion test was applied in this experiment. The experiment was modeled after the one employed by Spainhour mentioned in the literature review. The type of accelerated corrosion test that is employed has been used in several research reports, as mentioned in the literature review. Using the principles of electrolytic corrosion, this experiment employs an anode, cathode, electrolyte, and a contact between the anode and cathode, which are all the necessary components for corrosion to occur. The experimental procedure is detailed in the following sections.

3.2 Specimen Preparation

In total, there were forty-two specimens used for this experiment. The specimens were 2" by 4" cylinders with a single #4 rebar protruding from the center. This is known as a "lollipop" sample, and is commonly used in accelerated corrosion tests that examine reinforced concrete corrosion. The small sample dimensions were chosen in order to ensure corrosion would occur in a short period of time through the use of minimal concrete cover. Two concrete mixes were utilized in the testing; a lightweight concrete, and a similarly proportioned normalweight concrete. The mix for the lightweight concrete was determined first, after which a normalweight concrete mix was produced by exchanging the coarse lightweight aggregates for normalweight aggregates. The sand, water, and cement contents of the two mixes were kept identical; that way, only the type of coarse aggregate differed in the mix designs.

3.2.1 Concrete mix materials

The lightweight aggregate used was Streetman aggregate donated by the Expanded Shale, Clay and Slate Institute (ESCSI). Streetman is an expanded shale that has been used in Texas for double-tee members for parking garages (Heffington, 2000). The aggregates received were well graded with 3/4" maximum size.

The normalweight aggregate was crushed stone available outside the Civil Engineering Lab Building at the University of Texas at Arlington in storage bins. The bin contained both coarse and fine aggregates with a great range of sizes. In order to remove the fine aggregate and obtain coarse aggregates similar in size and grade to the lightweight aggregate for mixing, gradation using wire mesh sieves took place. Figures 3-1 and 3-2 show samples of the Streetman aggregate and the crushed stone aggregate, respectively.

Figure 3-1 3/4" Expanded Shale Streetman Aggregate from ESCSI

Figure 3-2 Normalweight Aggregates from UTA stock, sieved to 3/4" maximum size

As mentioned before, fine lightweight aggregates were not considered, so concrete sand was used for all of the fine aggregates in the mixes. The concrete sand from the UTA materials bins were used for this. Portland Type II Cement donated by Lehigh Hanson and standard tap water were the other components of the mixes.

3.2.2 Concrete mix design

3.2.2.1 Design considerations

To determine proportions for the mix design, ACI 211.2-98 (2004), the *Standard Practice for Selecting Proportions for Structural Lightweight Concrete*, was consulted. This practice gives approximate values for the different components of concrete depending on desired properties such as slump, compressive strength, etc. Most concretes used for structural purposes where corrosion would be an issue, such as in bridges or in parking garage members where deicing salts are used, generally have a compressive strength of at least 4000 psi, so this was a target strength for this experiment. A slump of 3 inches was desired to provide good workability during mixing. The concrete density for sand-lightweight concrete ranges from 105-120 lb/ft^3 in commercial projects. ACI 211.2-98 (2004) suggests a water cement ratio of no more than 0.40 for concrete clear cover of less than 1 in when exposed to sea water or sulfates, whereas the concrete in this experiment had a maximum clear cover of 0.75 in. It was desired to make a concrete that would corrode fairly easily in order to determine the corrosion protection effects of FRP, however, so a higher w/c ratio of approximately 0.45 was targeted.

Structural lightweight concrete for use in environments where corrosion is an issue generally contains mineral admixtures, such as silica fume or fly ash, to provide high strength and corrosion resistance. These admixtures have been shown to significantly reduce the permeability of lightweight concrete and increase their

mechanical properties. These admixtures were not considered for this experiment, however. There were a few reasons for this. For this experiment, the primary purpose was to determine what corrosion resistance effects FRP could provide to the lightweight concrete, so the addition of another corrosion protection system such as mineral admixture use would make it difficult to isolate the effects of the FRP. Also, it is much more difficult to corrode high strength concrete with admixtures, increasing the length of time to obtain meaningful results beyond the length of time desired. Finally, externally applied FRP is generally used for repair purposes, meaning it is used for damaged or deteriorated concrete. New concrete with mineral admixtures will usually not require FRP repair, and the corrosion protection effects of the FRP may be minimized.

Similar to the use of mineral admixtures is the use of air-entrainment and superplasticizers. Air entrainment is used to increase the total air content in concrete, which improves durability, workability, and reduces weight. Superplasticizer is used in high strength concrete to allow low w/c ratios to be used while still having enough workability. Neither of these were considered for the concrete mix design, so the mixes contained only aggregates, water, cement, and sand. The design can be found in Appendix A.

3.2.2.2 Concrete mixing

Using the design considerations above, the concrete was mixed through a trial-and-error method. The absorptive nature of lightweight aggregates require them to be soaked or sprinkled with water for a period of time prior to mixing to help ensure that water is not lost during the mixing process. The ideal condition is surface-saturated dry (SSD), however this is difficult to attain without determining the absorption percentage beforehand. Lightweight aggregates vary in how much water they absorb, and moisture content tests to determine aggregate absorption are considered unreliable for lightweight

aggregates (Heffington 2000). Lightweight aggregate manufactures recommend sprinkling water on the aggregate pile for 24 to 48 hours to approximate the SSD condition, however in the absence of sprinklers, the next best option is to submerge the aggregates in a tub for at least 24 hours and then let them dry to obtain a SSD condition. Heffington (2000) used this method, which was adopted for this experiment. The lightweight aggregates soaked in the tub for 48 hours before being allowed to dry in the sun and elements for a period of 20 to 30 minutes to allow the excess water to evaporate.

Figure 3-3 Lightweight Aggregates Soaking

Once the aggregate soaked and dried, the concrete was mixed. The mixing was done using a concrete mixer in the UTA lab, with the lightweight concrete mixed first. The appropriate amount of each material was measured out and placed in buckets. The lightweight aggregate and sand was mixed together first until a good mixture was appropriated. This was followed by the addition of cement and fly ash or silica fume if the mix required it. These components were all mixed thoroughly together. Next, the water

was added. All components were mixed thoroughly together. Figure 3-4shows the fresh mix.

Figure 3-4 Fresh lightweight concrete mix

After mixing, fresh properties of concrete were determined as detailed below, and cylinders for the accelerated corrosion testing and compressive strength tests were prepared. The same procedure was followed for the normalweight concrete, with the exception that the aggregates were not soaked beforehand.

3.2.2.3 Determination of concrete properties

Once the mixing was finished, the concrete was emptied into a wheelbarrow and tests to determine the fresh properties of concrete were carried out. These tests include the use of ASTM C138/138M for the fresh density of concrete, ASTM C143/143M for the standard slump test of concrete, and ASTM C173/173 for the determination of the air content of the concrete by the volumetric method. These are all standard tests that are commonly used to determine concrete properties.

Another property that must be determined for lightweight concrete alone is the equilibrium density. Since lightweight concrete absorbs water, the fresh density of lightweight concrete will be heavier initially then it will in service after a period of time. Some water will be lost due to evaporation from drying or internal curing, and so the concrete will reach a condition between oven-dry and saturated in which it is likely to operate at in service. This is equilibrium density, which is determined by ASTM C567. To approximate this condition through measurements, the ASTM requires 6 in x 12 in cylinders to be submerged for 24 hours in water at 23 ± 2^{o} C (73.5 ± 3.5^{o} F) after being removed from their molds 7 days after curing begins. The mass of these cylinders is measured, and then they are dried in a controlled humidity enclosure for a period of time and the mass measured until the difference in measurements is less than 0.5%. Oven-dry density is another condition that can be measured for lightweight concrete. This is done by removing the cylinders from their molds after 24 hours and submerging them in water. The mass of these submerged cylinders is measured. The cylinders are then removed from submersion, dried and drained, and measured in a saturated surface dry condition. They are then placed in an oven at 110 ± 5^{o} C (230 ± 9^{o} F) and dried for 72 hours. After the cylinders cool for 30 minutes, the mass is measured, and the process is repeated until successive mass measurements differ by less than 0.5%.

Measuring these properties for lightweight concrete can be very time consuming, so ASTM C567 allows the determination of an approximate oven dry and equilibrium density through the use of equations, if the mixture quantities and volume of concrete produced is known. These equations were used for the determination of equilibrium density in this experiment. The procedure and calculations for this determination can be found in Appendix A. The full properties of the lightweight and concrete produced are summarized in the following table.

Table 3-1 Concrete Properties

Concrete Properties					
	28-day f'c	Fresh Concrete Density	Equilibrium Density	Slump	Air content
	psi	lb/ft^3	lb/ft^3	in	%
LW	3820	121.54	116.77	2.6	2.6
NW	4200	144.45	N/A	2.4	3.1

3.2.2.4 Reinforcing Bars

The reinforcing bars (rebars) used to reinforce the cylinders were standard #4 rebars. Several four foot pieces of rebar were obtained and cleaned to remove as much surface rust as possible. They were then cut into 4" long pieces using a circular power saw. Forty two separate pieces were cut and were labeled with a number from 1 to 42. These rebars were then weighed.

One rebar was placed into each of the forty-two 2" by 4" cylinders. Due to the small sizes of the cylinders, the rebars were placed as closed to the center of the cylinder as possible. This gave a uniform 3/4" concrete cover on the sides. Initially, it was desired for the rebar to protrude 3/4" from the top of the cylinder to give a concrete clear cover of 3/4" from the bottom of the cylinder. This was difficult to achieve, however. The concrete placed in the cylinders was consolidated using a shaker table, as rodding would prove difficult for the small dimensions in the 2" by 4" cylinders. When vibrating lightweight concrete, the aggregates tend to float to the top of the cylinder. This caused the rebar to settle a bit, to a clear cover of approximately 1/2". Several of the cylinders had this tendency, so it was decided to make the 1/2" cover standard throughout all of the cylinders. There were a few cylinders, however, that had 3/4" cover due to the rebar resting directly on a large piece of aggregate. It was noted which cylinders had this

different cover to see if it had any effect during the corrosion testing. Another few select cylinders had a clear cover of 1/4", and these cylinders were also noted.

After the concrete and rebar were placed in the cylindrical molds, the cylinders were placed in a curing chamber to cure for 28 days at an approximate temperature of 85^{o} F (29.44^{o} C) and 100% relative humidity. Six 4" by 8" cylinders were created to determine the compressive strength of the concrete, as specified by ASTM C39/39M. Three of these cylinders were cast for the lightweight concrete mix, and the other three for the normalweight concrete mix. After the concrete had cured for 28 days, they were removed from the curing chamber so that the FRP could be applied. The FRP properties and application procedure will be detailed in the next section. Figure 3-5 shows the concrete curing in the chamber.

Figure 3-5 Concrete in the curing chamber

3.2.3 FRP application

3.2.3.1 FRP properties

After the specimens finished curing for 28 days, they were removed from the chamber and wrapped with FRP. Three different FRP systems were utilized for the wrapping. The first system is the Tyfo SEH-51A System, a Glass FRP from Fyfe Co. This is a custom weave, unidirectional glass fabric oriented in the 0^{o} direction with additional yellow glass cross fibers at 90^{o}. It utilizes the Tyfo S epoxy, which is a two component epoxy system. Both the epoxy and FRP were leftover materials, and were a year old at the time of this experiment .Some advantages of the system according to the product sheet are good high & low temperature properties, long working time, high elongation, ambient cure, and 100% solvent free (FyfeCo, LLC). The typical dry fiber properties, composite gross laminate properties, and epoxy material properties are shown in Tables 3-2 and 3-3. These properties are taken directly from the product sheet available on Fyfe's website.

Table 3-2 Dry Fiber Properties of Tyfo SEH-51A (FyfeCo, LLC)

Typical Dry Fiber Properties			
Tensile Strength		470,000 psi (3.24 GPa)	
Tensile Modulus		10.5×10^6 psi (72.4 GPa)	
Ultimate Elongation		4.5%	
Density		0.092 lbs./in.^{3} (2.55 g/cm^3)	
Minimum weight per sq. yd.		27 oz. (915 g/m^2)	
Composite Gross Laminate Properties			
PROPERTY	**ASTM METHOD**	**TYPICAL TEST VALUE**	**DESIGN VALUE***
Ultimate tensile strength in primary fiber direction	D3039	83,400 psi (575 MPa) (4.17 kip/in. width)	66,720 psi (460 MPa) (3.3 kip/in. width)
Elongation at break	D3039	2.2%	1.76%
Tensile Modulus	D3039	3.79×10^6 psi (26.1 GPa)	3.03×10^6 psi (20.9 GPa)
Ultimate tensile strength in 90 degrees to primary fiber	D3039	3,750 psi (25.8 MPa)	3,000 psi (20.7 MPa)
Nominal Laminate Thickness		0.05 in. (1.3mm)	0.05 in. (1.3mm)

* Gross laminate design properties based on ACI 440 suggested guidelines will vary slightly. Contact Fyfe Co. LLC engineers to confirm project specifications values and design methodology

Table 3-3 Tyfo S Epoxy Properties (FyfeCo, LLC)

Epoxy Material Properties		
Curing Schedule 72 hours post cure at 140° F (60° C).		
PROPERTY	**ASTM METHOD**	**TYPICAL TEST VALUE***
Tensile Strength[1], psi	D638 Type 1	10,500 psi (72.4 MPa)
Tensile Modulus, psi	D638 Type 1	461,000 psi (3.18 GPa)
Elongation Percent	D638 Type 1	5.0%
Flexural Strength, psi	D790	17,900 psi (123.4 MPa)
Flexural Modulus, psi	D790	452,000 psi (3.12 GPa)
T_g	D4065	180° F (82° C)
[1] Testing temperature: 70° F (21° C). Crosshead speed: 0.5 in. (13mm)/min. Grips Instron 2716-0055 - 30 kips.		

* Specifications values can be provided upon request.

The second system used was the Tyfo SCH-41 System, also from Fyfe. This is a Carbon FRP, comprise of Tyfo S Epoxy and Tyfo SCH-41 reinforcing fabric. It is a custom, uni-directional carbon fabric orientated in the 0^o direction. It's advantages include improved long-term durability, good high & low temperature properties, long working time, high tensile module and strength, ambient cure, and 100% solvent free (Fyfe Co, LLC). The same leftover epoxy was used, however this Carbon sheet was a new sheet donated by Fyfe. Table 3-4 shows its typical dry fiber properties and composite gross laminate properties.

Table 3-4 Properties of Tyfo SCH-41 System (Fyfe Co, LLC)

Typical Dry Fiber Properties			
Tensile Strength		550,000 psi (3.79 GPa)	
Tensile Modulus		33.4 x 10^6 psi (230 GPa)	
Ultimate Elongation		1.7%	
Density		0.063 lbs./in.^{3} (1.74 g/cm^3)	
Minimum weight per sq. yd.		19 oz. (644 g/m^2)	
Composite Gross Laminate Properties			
PROPERTY	**ASTM METHOD**	**TYPICAL TEST VALUE**	**DESIGN VALUE***
Ultimate tensile strength in primary fiber direction	D3039	143,000 psi (986 MPa) (5.7 kip/in. width)	121,000 psi (834 MPa) (4.8 kip/in. width)
Elongation at break	D3039	1.0%	0.85%
Tensile Modulus	D3039	13.9 x 10^6 psi (95.8 GPa)	11.9 x 10^6 psi (82 GPa)
Flexural Strength	D790	17,900 psi (123.4 MPa)	15,200 psi (104.8 MPa)
Flexural Modulus	D790	452,000 psi (3.12 GPa)	384,200 psi (2.65 GPa)
Longitudinal Compressive Strength	D3410	50,000 psi (344.8 MPa)	42,500 psi (293 MPa)
Longitudinal Compressive Modulus	D3410	11.2 x 10^6 psi (77.2 GPa)	9.5 x 10^6 psi (65.5 GPa)
Longitudinal Coefficient of Thermal Expansion	D696	3.6 ppm./°F	
Transverse Coefficient of Thermal Expansion	D696	20.3 ppm./°F	
Nominal Laminate Thickness		0.04 in. (1.0mm)	0.04 in. (1.0mm)
* Gross laminate design properties based on ACI 440 suggested guidelines will vary slightly. Contacted Fyfe Co. LLC engineers to confirm project specifications values and design methodology			

The tables above show the SEH-51A glass reinforcing fabric and SCH-41 carbon reinforcing fabric, respectively. These are the composite laminates before being saturated with epoxy and applied to the concrete, as detailed in the next section.

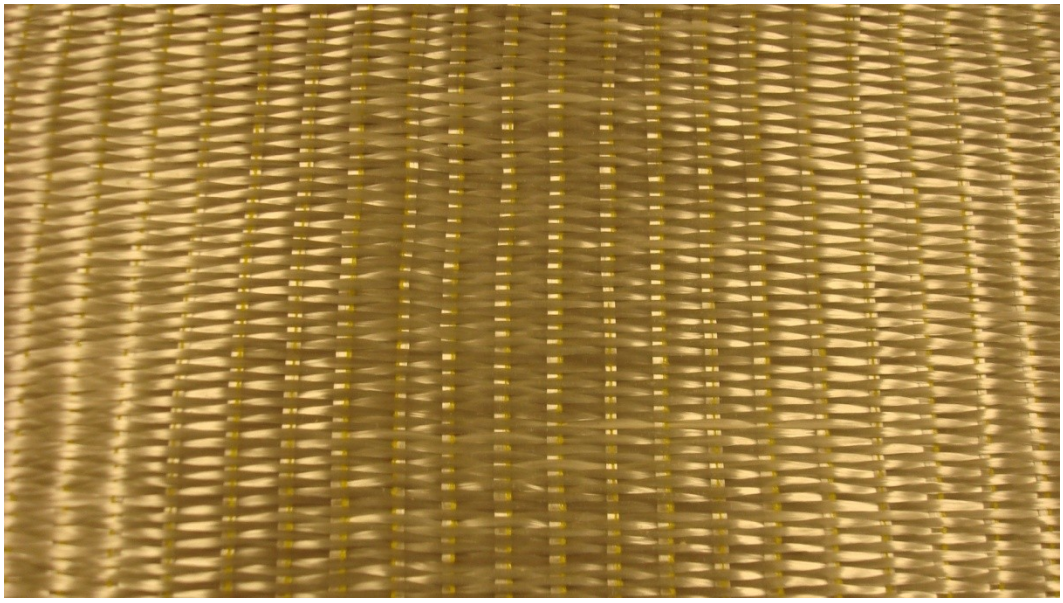

Figure 3-6 Tyfo SEH-51A Glass Composite Laminate

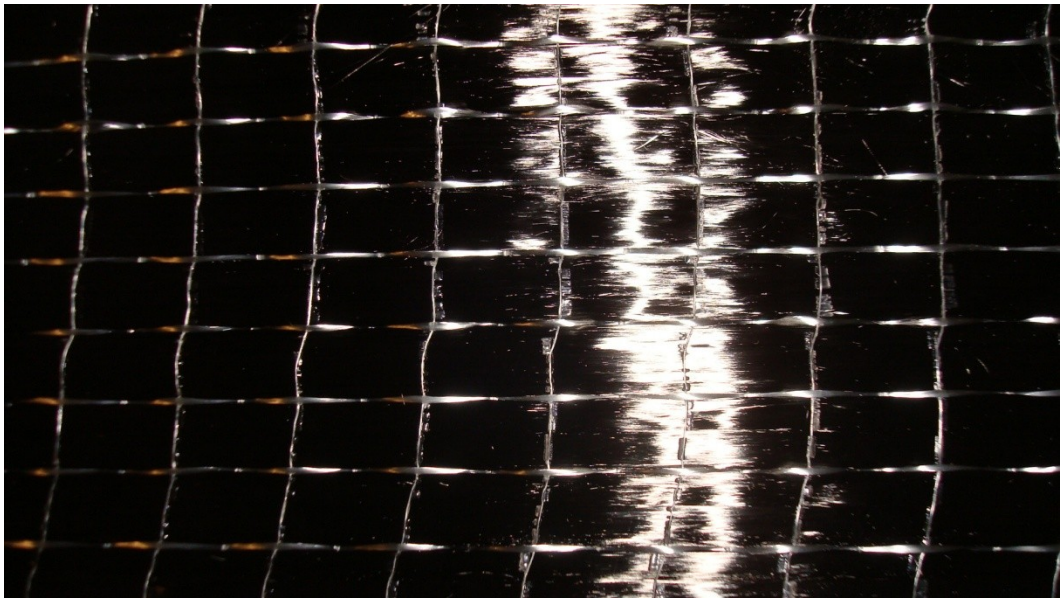

Figure 3-7 Tyfo SCH-41 Carbon Composite Laminate

The final FRP system used was another CFRP system, this one from Sika corporation. This system utilized the SikaWrap Hex 103C carbon fiber composite, which is a high strength, unidirectional composite. The properties of the laminates are shown below.

Table 3-5 Typical Properties for Sika Hex 103 C system (Sika Corporation)

Typical Dry Fiber Properties			
Tensile Strength		550,000 psi (3.79 GPa)	
Tensile Modulus		34 x 10^6 psi (230 GPa)	
Elongation		1.5%	
Density		0.063 lbs./in.^{3} (1.74 g/cm^3)	
Weight per sq. yd.		18 oz. (618 g/m^2)	
Cured Laminate Properties with Sikadur Hex 300 epoxy Properties after standard cure followed by standard post cure. [70°-75°f (21°-24°C) - 5 days and 48 hour post cure at 140°f (60°C)]			
PROPERTY	**ASTM METHOD**	**AVERAGE VALUE[1]**	**DESIGN VALUE[2]**
Tensile Strength*	D3039	123,200 psi (986 MPa)	104,000 psi (834 MPa)
Tensile Modulus*	D3039	10.2 x 10^6 psi (70.55 GPA)	9.45 x 10^6 psi (65 GPa)
Tensile % Elongation*	D3039	1.12%	1.12 %
140° F - Tensile Strength	D-3039	123,000 psi (847 MPa)	101,400 psi (699 MPa)
140° F - Tensile Modulus	D-3039	10.14 x 10^6 psi (69.84 GPA)	9.156 x 10^6 psi (63.088 GPa)
Compressive Strength	D-695	113,000 psi (779 MPa)	103,800 psi (715 MPa)
Compressive Modulus	D-695	9.73 x 10^6 psi (67.01 GPa)	8.93 x 10^6 psi (61.5 MPa)
90 deg Tensile Strength	D-3039	3500 psi (24 MPa)	2300 psi (16 MPa)
90 deg Tensile Modulus	D-3039	705,500 psi (4,861 MPa)	576,700 psi (3,973 MPa)

Table 3-5 *continued*

90^{o} deg % Tensile Elongation	D-3039	0.45	0.33
Shear Strength +/- 45 in. Plane	D-3518	7500 psi (52 MPa)	6,700 psi (46 MPa)
Shear Modulus +/- 45 in. Plane	D-3518	362,500 psi (2498 MPa)	347,500 psi (2394 MPa)
Ply Thickness (inch/mm)	0.04	1.016	
Tensile Strength per inch width	D-3039	4928 lbs (21.9 kN)	4160 lbs (18.5 kN)

* 24 sample coupons per test series; all other values based on 6 coupon test series

[1] 1 Average value of test series

[2] 2 Average value minus 2 standard deviation

Table 3-6 Typical Epoxy Properties (Sika Corporation)

Mechanical Properties (14 day cure @73°F (23°C) and 50% R.H.)			
PROPERTY	**ASTM METHOD**	**AVERAGE VALUE**	
Tensile Strength	D-638	8000 psi (55 MPa)	
Tensile Modulus	D-638	2.5×10^{6} psi (1724 MPA)	
Elongation @ Break	D-638	3%	
Flexural Strength	D-790	11,500 psi (79 MPa)	
Flexural Modulus	D-790	5×10^{6} psi (3,450 MPa)	

The Sika FRP and epoxy were brand new, as opposed to the Fyfe products which were over a year old when they were used in this experiment. Due to this, the

mechanical properties of the Tyfo-S epoxy had most likely diluted, whereas the Sika products would have more of their full potential for use.

3.2.3.2 FRP wrap configurations and specimen labeling

Several FRP configurations used for both lightweight and normalweight concrete were utilized for this experiment. Three cylinders were used for each separate configuration to help ensure the data collected was consistent among multiple samples. The variables in the configurations included the type of concrete (lightweight or normalweight), the type of FRP (GFRP or CFRP, Fyfe or Sika), and the number of layers of FRP applied (one or two). To keep track of these different configurations a labeling system was used to refer to specific samples. This system utilizes a LW or NW for lightweight concrete or normalweight concrete, respectively; G or C for glass or carbon FRP; F or S for Fyfe or Sika;1L or 2L for the number of wraps used; and 1,2, or 3 for the sample number. For example, LW-G-F-1L-1 is the first sample of a lightweight concrete cylinder wrapped with 1 layer of Fyfe GFRP. For the control samples, they are simply labeled as LW or NW Control 1, 2, or 3.

Table 3-7 lists the different configurations. The first column has a number from 1 to 42; this number indicates the number assigned to the rebar used in the sample. The second column is the FRP configuration.

Table 3-7 FRP Configurations

Rebar number and FRP configuration used			
1	LW Control 1	22	NW Control 1
2	LW Control 2	23	NW Control 2
3	LW Control 3	24	NW Control 3
4	LW - G- F- 1L - 1	25	NW - G - F- 1L - 1
5	LW - G - F- 1L - 2	26	NW - G - F- 1L - 2
6	LW - G - F- 1L - 3	27	NW - G - F- 1L - 3
7	LW - G - F- 2L - 1	28	NW - G - F- 2L - 1

Table 3-7 *continued*

8	LW - G - F- 2L- 2	29	NW - G - F- 2L - 2
9	LW - G - F- 2L - 3	30	NW - G - F- 2L - 3
10	LW - C - F- 1L - 1	31	NW - C - F- 1L - 1
11	LW - C - F- 1L - 2	32	NW - C - F- 1L - 2
12	LW - C - F- 1L - 3	33	NW - C - F- 1L - 3
13	LW - C - F- 2L - 1	34	NW - C - F- 2L - 1
14	LW - C - F- 2L - 2	35	NW - C - F- 2L - 2
15	LW - C - F- 2L - 3	36	NW - C - F- 2L - 3
16	LW - C -S- 1L - 1	37	NW - C - S- 1L - 1
17	LW - C - S- 1L - 2	38	NW - C - S- 1L - 2
18	LW - C - S- 1L - 3	39	NW - C - S- 1L - 3
19	LW - C - S- 2L - 1	40	NW - C - S- 2L - 1
20	LW - C - S- 2L - 2	41	NW - C - S- 2L - 2
21	LW - C - S- 2L - 2	42	NW - C - S- 2L - 3

As mentioned before, a few of the samples contained different clear cover than the standard 1/2" cover. The samples with rebar 7 and rebar 34 had clear covers of 3/4 in. Samples 8 and 2 had 1/4" cover. These samples will be mentioned in the results section to explain if any differences due to cover could be discerned.

3.2.3.3 FRP wrapping procedure

The FRP wrapping followed a wet lay-up method recommended by the manufacturers. The samples with the Tyfo FRP were wrapped first following the procedures on the product sheet. The first step was to prepare the concrete substrates for all the samples. This involved roughing the concrete, which has been shown to improve the bond between the epoxy and concrete. Roughing the concrete was achieved using a small handheld grinding tool, which was slowly used around the entirety of each sample to ensure adequate roughing. After the grinding was completed, the samples were cleaned and dried to make sure any foreign substances that could interfere with the bond were removed.

Following the surface preparation, the FRP sheets were cut to the desired lengths to be able to wrap around the entire cylinder. The sheets were cut into strips of 4 in by 8 in dimensions, in order to wrap around the full height of the cylinder and around the circumference. The sheets were made sure to be long enough so that when they wrapped around the cylinder there would be an overlap of at least 1 in; this would help ensure that delamination,, in which the FRP becomes detached from the surface it is being applied to, would be minimized. For cylinders with multiple layers of FRP, the second layer had to be slightly longer than the first due to the added circumference the first layer created on the sample.

Once the samples were prepared and the sheets cut, the FRP application process could begin. First the epoxy had to prepared. The Tyfo S epoxy is comprised of two components which must be mixed together. The mix comprises of 100 parts of Component A to 34.5 parts of Component B by weight. Approximately three pounds of epoxy were mixed, using 2.2 pounds of component A and 0.76 pounds of component B. Only low amounts of epoxy were needed for the small cylinders used, so a small mixer was used. The mixer ran for 5 minutes at 400 rpm until a uniform blend was observed. After this was done, one quarter of this mixture was removed and placed in a small container. Silica powder was added to this portion at approximately 7% by weight and mixed together by hand. The purpose of this thickened epoxy is to fill any voids in the concrete substrate so that FRP bonding can occur over an even surface. After the epoxy was prepared, the FRP was applied to the cylinders one at a time. First a priming coat of the epoxy without the silica was applied on the sides and bottom of the sample using a roller; the top of the cylinder where the rebar was protruding was left untreated. A layer of the thickened epoxy was then applied over the priming layer to fill the voids in the concrete. The FRP fabric was saturated on both sides with several coats of the epoxy so

that it seeped all the way through the fibers. Pressure was applied using the roller to make sure the entire fabric was saturated. The FRP was then slowly and carefully wrapped around the cylinder, utilizing hand pressure between the fabric and the concrete so that a good bond could take place.

FRP is a very stiff material, so before it cures the ends of the material have a tendency to try to separate from the concrete. For larger samples this separation is not as pronounced, but for the small samples used in this experiment the FRP would not stay bonded without applying constant pressure while it cured. Therefore, two or three rubber bands were used to constrict the FRP so that it would be forced to bond to the concrete. Some of the epoxy became attached to the rubber bands, so they were left on the samples throughout the experiment so that the epoxy would not be stripped.

After the FRP was applied and constricted so that it would not separate, another coat of epoxy was applied. If multiple layers of FRP were used, the second layer was saturated and applied over the first layer. Rubber bands were applied again to prevent separation. Both the Tyfo SEH-51A and SCH-41 systems were applied using this procedure.

The SIkaDur epoxy was mixed similarly to the Fyfe, except a ratio of 1:1 for components A and B were mixed as according to the directions of the manufacturer. The silica was also used for this application in the same amount as for the Tyfo-S epoxy.

After all of the samples were wrapped, they were left undisturbed to cure for 48 hours. The Tyfo samples were wrapped first and cured for approximately 4 or 5 days before the Sika FRP and epoxy were available in the laboratory to use. Therefore, the Tyfo wrapped samples had more time to cure than the Sika wrapped samples. The Sika samples were able to cure for 48 hours, and after enough time had elapsed all 42 samples were placed in a plastic tank to begin the accelerated corrosion test.

3.3 Accelerated Corrosion Test

3.3.1 Background on the test

As mentioned before, corrosion can take place with the presence of an anode, a cathode, an electrolyte, and an electrical contact path between two different metals. This is known as galvanic corrosion. Electrolytic corrosion is similar to galvanic corrosion except that the current is produced by an external power source. This type of corrosion forms the basis for this experimental setup. This type of setup has been used in several accelerated corrosion tests, as mentioned in the literature review.

Galvanic corrosion occurs when two dissimilar metals are in contact, which creates a galvanic cell. The potential difference between the two metals in this cell creates a current from the anode through the electrolyte to the cathode, then back to the anode through the electric path (AWWA, 2002). The more noble metal in this cell becomes the cathode, in which electrons are consumed, whereas the less noble metal becomes the anode, where electrons are produced. Therefore, the flow of electrons is from the anode to the cathode. The loss of electrons in the rebar leaves positively charged atoms that combine with oxygen and moisture to form hydroxyl ions, which combine with ferrous ions to form ferrous hydroxide and ferrous oxide (Spainhour, 2002). Ferrous oxide and ferrous hydroxide occupy greater volumes than what they were created with, which creates radial pressures causing cracking.

When two metals create a galvanic cell, they create their own current. In electrolytic corrosion, a direct current from an external source can drive the corrosion reaction by supplying the current in the electric return path. These external currents, known as stray currents, are generally much stronger than the ones produced in the galvanic cell and may cause corrosion much faster (Smiths Power, 2013).

With these principles in mind, the accelerated corrosion test for this experiment makes use of an anode, cathode, electrolyte, contact path, and direct current from an external source to quickly induce corrosion.

3.3.2 Test Setup

Once all forty two samples were finished curing, the experiment was set up. This experiment was based on the one by Spainhour et. al. (2003). The samples were placed in a plastic tank with dimensions of 35-5/8" x 18-1/4" x 6-1/4". The specimens would be submerged up to approximately 3 - 1/4" of a 5% by weight salt solution. This solution was made by combining distilled water with ordinary table salt. The concentration of salt is stronger than that found in seawater (about 5%), but would ensure a steady flow of electrons to the samples so that corrosion would occur.

A Vellemans DC Power Supply was used to provide a direct current through the system. This power supply had a maximum capacity of 15 V and 3 amps. Figure 3-8 shows the power supply.

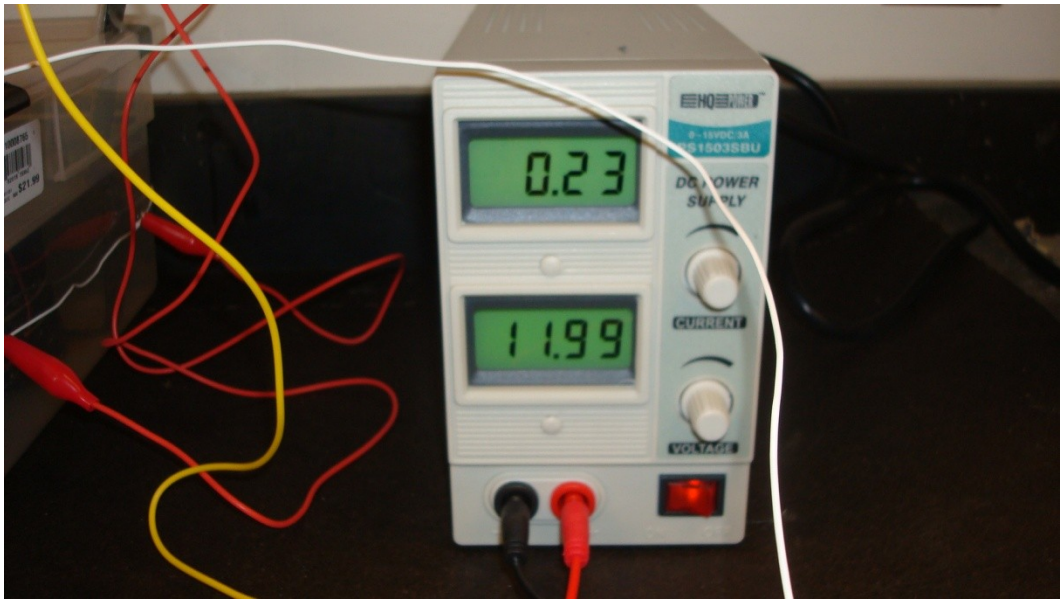

Figure 3-8 DC Power Supply

To move the applied current through the samples, 20-gauge copper bell electric wires were used. The samples were wired in a parallel configuration so that the current flow would not be interrupted as individual samples failed and were removed from the tank. The circuit began at the positive terminal of the DC Power Supply. A banana plug was inserted into the positive terminal and a large alligator clip at the other end was attached to a wire running the length of a 4 foot piece of plywood. For every individual sample, another exposed wire was wrapped around the first wire and attached to one of the screw terminals of a toggle light switch. A third wire extended from the other screw terminal to a 10-ohm resistor to help protect the electric circuitry, and a fourth wire extended from the resistor and wrapped around the embedded rebar. To complete the circuit, the current would travel through the anode, into the electrolytic salt solution and through the cathodes, where alligator clips connected them to another long wire wrapped around the tank. Another large alligator clip attached to the exposed portion of this wire, which ended in a banana plug inserted into the negative end of the power supply.

Figure 3-9 Experiment Setup

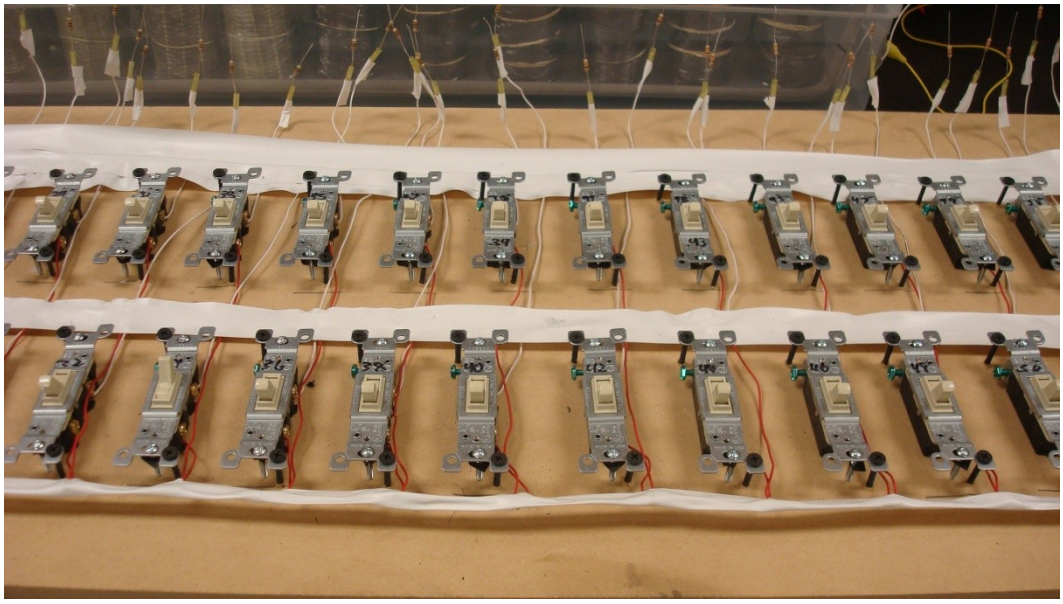

Figure 3-10 Wiring in parallel

Figure 3-11 Samples completely wired and partially submerged in salt solution

Stainless steel blanks were used for the cathodes in this experiment. This is a nobler metal than the carbon-steel rebars, so the current flows to the rebar, inciting corrosion. Three stainless steel blanks, 1/8 inches thick, 1 in wide and 6 feet long, were

placed in the tank equally spaced apart. They were bent in a fashion so that they would conform to the shape of the tank, so they laid flat along the bottom of the tank and rose at the sides. The alligator clips were attached to the ends of these blanks and connected to another wire for electricity to flow.

The use of light switches enabled individual electric paths to be opened or closed based on the position of the switch. This would allow current measurements to be taken in individual samples. The amount of current flowing through is an indicator of corrosion, as seen through the use of Faraday's Law in which mass loss of a metal can be seen proportional to the current. Faraday's Law will be examined in greater detail in the Results section where theoretical mass loss and actual mass loss will be compared.

After the test was setup and everything properly wired, the test could begin. Since the wiring was done in parallel, the voltage in each component of the circuit would be equal, i.e. $V=V_1=V_2=...=V_n$. Therefore, a constant voltage was applied from the power supply to the samples for the length of the test. It was decided to use a constant 12 volts. This voltage was high enough that corrosion could occur in a relatively short amount of time, yet low enough so that overheating of the 10 ohm resistors would be avoided. The test duration was set at 50 days. During this time, current measurements were taken every day. The electrical wiring was also checked daily to make sure that each sample had sufficient electricity running through them. Any burned out or corroded wires were replaced. Electrical tape was utilized to make certain that the wires would remain in constant contact with the rebar. Samples were checked for failures. Specific failures that were looked for included cracking in the concrete substrate with a corresponding current spike; delamination of the FRP from the concrete substrate; and failure in the FRP wrap itself in the form of ripping. An excessive localized current failure was also observed; this will be detailed in the results section. As samples failed, they were removed from the

tank for other tests to be performed, including rebar mass loss and chloride content. At the end of 50 days, any samples that did not fail were removed from the tank and also tested. Corrosion is a complex mechanism and there is no single test that can completely and accurately define the behavior of concrete under corrosion. Therefore, multiple tests and measurements are used to determine how systems are behaving when corroded. The methods used for this experiment are explained in the next few sections.

3.3.3 Current Measurements

The applied 12 volts is constant across the parallel components of the circuit created, however the current will vary Current flows because a potential difference (voltage) exists between two metals relative to the electrolyte (Norton Corrosion Limited). Therefore, as the electrolytic salt solution breaks through the FRP layers and comes in contact with the rebar, an electrical path occurs between the rebar and stainless steel. This path allows the current to flow from the anode to the cathode as the system tries to protect the cathode. High current measurements indicate that corrosion is taking place as the salt solution is able to reach the anode and create the electrical path. The salt water solution and DC current allow this process to occur much more quickly than it would in nature.

The different FRP configurations provides a barrier from the electrolyte, so lower values of current measurements mean that the FRP system is still protecting the rebar. The different configurations provide varying levels of protection from the electrolytic salt solution, which the current levels help to indicate.

For this reason, current measurements were taken every day to give an indication of occurring corrosion. To take current measurements, an ammeter was used. This ammeter has to become a part of the system itself, connected in series, in order to obtain current readings. This was accomplished in this experiment by disconnecting the

DC power supply from the system and connecting the ammeter in its place. Following that, current measurement for individual samples were taking by turning all of the switches to the off position except for the sample presently being checked. Once that measurement was taken, it was switched to the off position and the next switch was turned to the on position, repeating until all the measurements were taken and recorded.

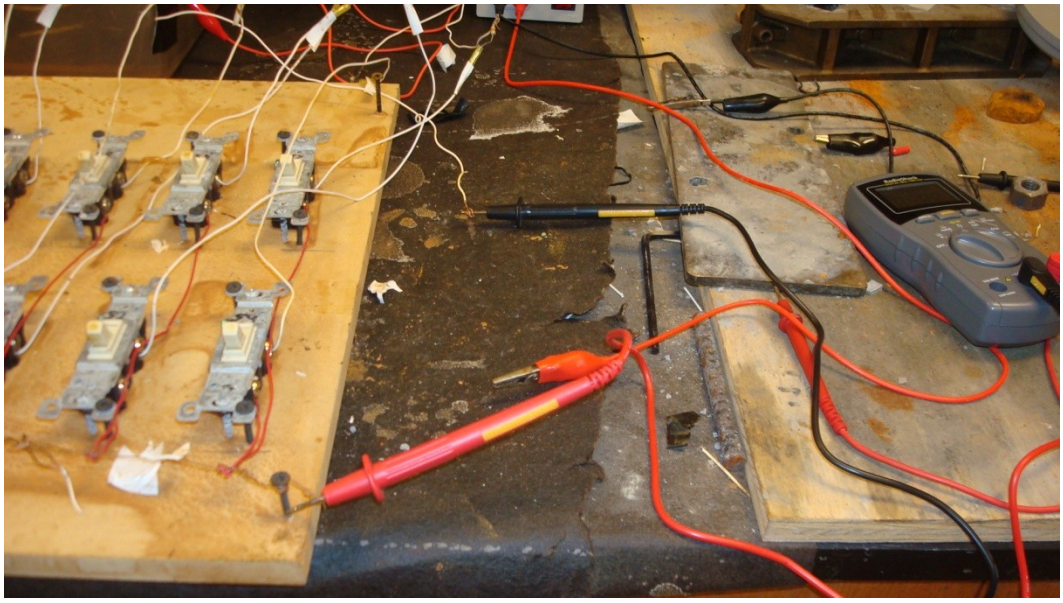

Figure 3-12 Ammeter connected as part of the circuit

During the accelerated corrosion process, as cracks in the concrete propagated, current readings would correspondingly become larger as more paths for the electrolyte to flow to the rebar were being created. Thus, a rapid increase or spike in current would generally be followed by visible cracking in the specimen. Once this occurred the specimen was removed from the tank as it had failed.

3.3.4 ASTM C1152 - Standard Test Method for Acid-Soluble Chloride in Mortar and Concrete

After specimens were removed from the tank they were subject to further analysis. One form of analysis was the determination of the activity of chlorides in the concrete. The ability to measure the penetrability of chloride ions by measuring electrical charge or determining the chloride content through chemical analysis can be used as a measurement of corrosion activity. Due to the fact that these cylinders are wrapped with FRP, chloride penetration tests that use electrical indication for penetration are difficult to perform. For instance, ASTM C1202 is the Standard Test Method for Electrical Indication of Concretes Ability to Resist Chloride Ion Penetration. This test is commonly used as a quick indicator of chloride penetration. It involves applying a DC voltage to a cylindrical specimen placed between two reservoirs; one filled with a 3% NaCl solution and the other with a 0.3 M NaOH solution. The voltage is applied and the total charge is measured after 6 hours. The test, however, requires specimens of 4 in diameter and 2 in thickness. Due to the fact that the cylinders in this experiment are 2 in diameter specimens, the requisite thickness would not be attainable with these cylinders. Another issue with the test is that it depends on the conductivity of the materials, so a highly conductive material such as carbon FRP will give results that are erroneously high (Stanish et. al., 1997).

It was determined for this experiment that the best way to find the ability of the FRP to resist chloride penetration was to determine the chloride content using a chemical titration analysis. ASTM C1152 is the Standard Test Method for Acid-Soluble Chloride in Mortar and Concrete. This test measures the amount of chloride in a concrete or mortar system with nitric acid to free the acid-soluble chloride in the system and then measuring the amount of chloride using a chemical titration. This method is useful for determining

the effectiveness of admixtures or protection systems such as FRP in reducing chloride penetration in one sample of concrete. However, this test method is not useful for comparing different concrete mixes that utilize different aggregates, since the amount of acid-soluble material is different. In this particular experiment, the lightweight aggregate used in not acid-soluble, so the acid-soluble chloride is restricted to the cement faction of the concrete. What this test was intended to do for this experiment is compare the effectiveness of the different FRP systems and FRP configurations for each mix. Therefore, the lightweight concrete control samples were compared to the wrapped lightweight samples, and the wrapped samples were compared to each other. The same comparison was made for the normalweight samples. No direct comparison was made between lightweight and normalweight samples.

The concrete samples were drilled using a handheld drill. The cylinders were drilled at the center of the sides of the sample, 2 inches from the top and bottom of the cylinder, to a depth of 3/4", or to the location of the face of the rebar. This location was chosen because all of the cylinders had a cover of 3/4" on the sides, while some of the rebars had variable concrete cover from the bottom of the cylinder. The test requires gathering 20 grams of a sample and testing 10 grams. To get enough material, different drill bit sizes had to be used. Before each sample of material was gathered, the drill bits were cleaned with isopropyl alcohol to avoid contamination. A 1/8" drill bit was used first, where the first 0.5 grams of material was discarded. The hole was drilled to the rebar, then a 3/8" drill bit was used to widen the hole. Again, the first 0.5 grams of material was discarded, then the rest collected. Finally, a 5/8" drill bit was used until enough material was gathered. Another 10 grams of sample was obtained at the same location on the opposite side of the cylinder using the same method. The sample was pulverized and

sieved through a No. 20 sieve so that large pieces of concrete and bits of FRP were removed from the sample.

To begin the titration process, 10 grams of sample was placed in a 250 mL beaker. The samples were dispersed with 75 mL of reagent grade water and stirred with a glass rod. 25 mL of diluted nitric acid was added to the mix along with three drops of methyl orange indicator, followed by 3 mL of hydrogen peroxide. An observation for a consistent red or pink color above the settled samples was looked for; if it did not appear, nitric acid was added dropwise until the color was observed. This process was done for the normalweight concrete; for the lightweight concrete, it was nearly impossible to find a consistent red or pink color. Therefore, for the lightweight concrete, the process was continued until there was no visible acid reaction with the addition of more nitric acid. After this process the sample was boiled for 10 seconds and transferred to a 250 mL Buchner flask. The beaker was then rinsed with water, and the solution was transferred back to the beaker and allowed to cool. Following this, 2 mL of standard 0.05 N NaCl solution was put into the beaker with a pipette. The solution was ready to be titrated.

The solution was placed on a magnetic stirrer with a magnetic stir bar placed inside. A silver/sulfide electrode connected to a voltmeter was submerged into the solution. This sample was gradually titrated using a standard 0.05 N silver nitrate solution until the equivalence point was reached. A standard reading was first made by submerging the electrode in the 250 mL beaker filled with water only. The samples were titrated in increments of 0.20 mL until they were approximately 60 mV below this standard, then the amount of AgNo3 required to reach this point was recorded. The percent chloride by mass of concrete could then be calculated with the equation provided in the ASTM.

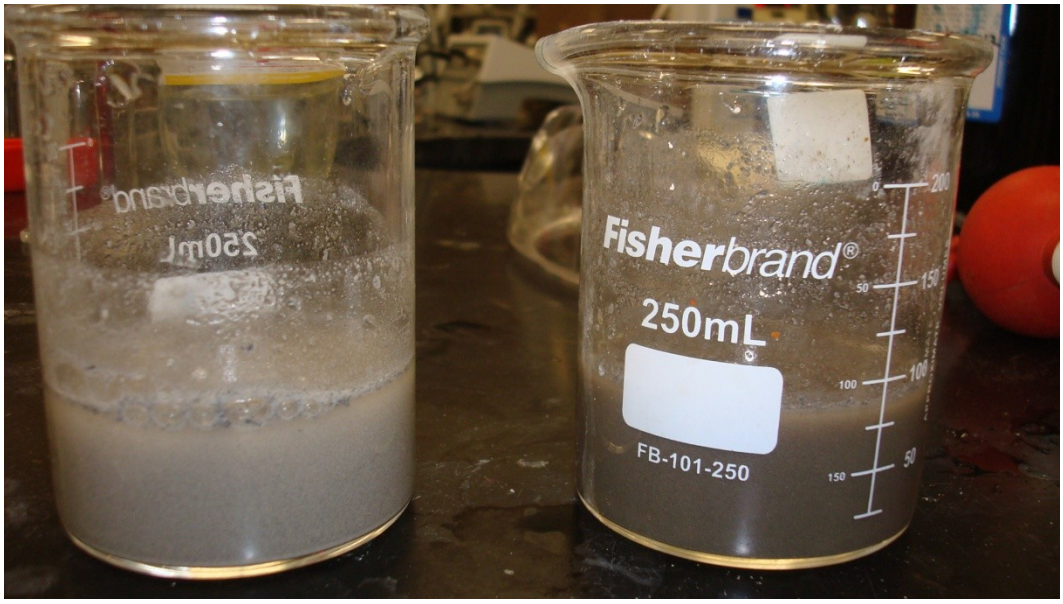

Figure 3-13 Concrete sample dispersed with water (NW on left, LW on right)

Figure 3-13 shows the concrete samples dispersed with water. The solution with the lightweight sample on the right of the figure is much darker than the NW solution. As mentioned earlier, the lightweight concrete did not readily display a red or pink color even when a great amount of acid was used. The nitric acid was added to the solution until any visible acidic reaction had ceased, which generally left the acid with a murky green to yellow color. The normalweight concrete, on the other hand, was able to demonstrate a red color as the nitric acid was added. Due to the fact that there was not a direct comparison between the two types of concrete, these methods were used in order to be consistent with each particular concrete. Figures 3-14 and Figures 3-15 show the appearance of a lightweight sample while cooling and a normalweight sample while being titrated, respectively.

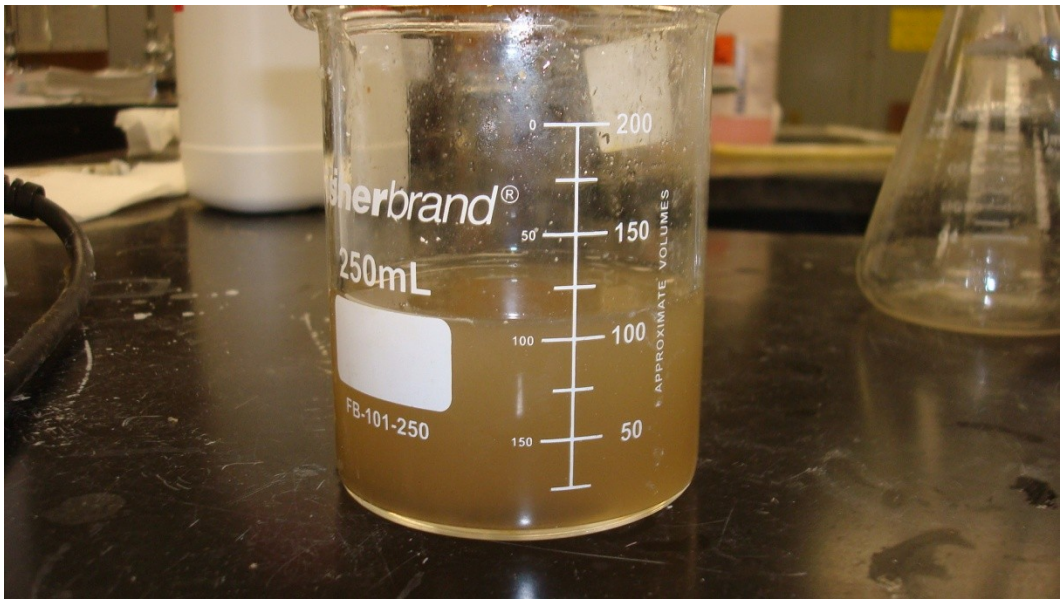

Figure 3-14 Lightweight Concrete sample cooling.

Figure 3-15 Normalweight Concrete titration

3.3.5 Rebar Mass Loss

After the samples were drilled for material for the chemical titration, the rebar was extracted to be weighed. The samples were carefully broken open with a hammer, and

the rebar was removed and placed into labeled plastic bags. To get an accurate weight of the rebar they were submerged in an acid solution. ASTM G1-03 was consulted for the acid to be used. The solution consisted of 1000 mL of 1.19 specific gravity Hydrochloric Acid, 20 grams of antimony hydroxide (Sb_2O_3), and 50 grams of Stannous Chloride (S_nCl_2), with all components well mixed together. This solution, at a temperature of 20 to 25^o C (68 to 77^o F), allowed the corrosion to be removed from the rebar in a period of 1 to 25 minutes.

Figure 3-16 Rebar submerged in acid

Figure 3-17 Rebar before corrosion removal

Figure 3-18 Rebar after corrosion removal

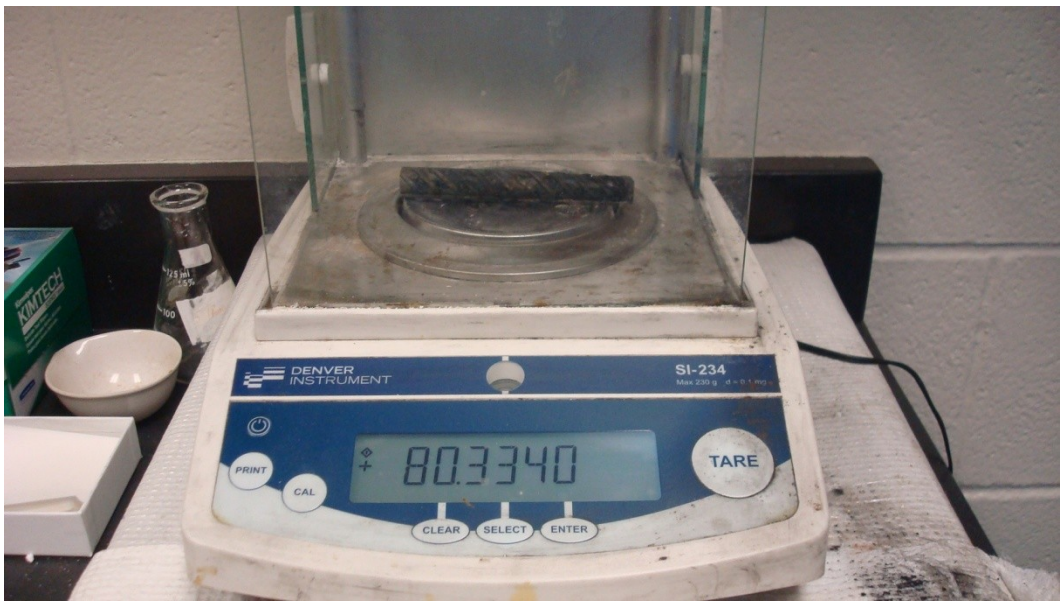

Figure 3-19 Weighing the cleaned rebar

After the corrosion products were removed from the rebar, the bar was removed from the acid, washed thoroughly with water, and dried with a towel. They were allowed to air dry to remove any remaining moisture, then they were weighed as shown in Figure 3-19. The weight was recorded to two decimal places. The percentage of mass loss was then calculated. The actual rebar mass loss was compared with the theoretical bar mass loss according to Faraday's Law.

Chapter 4

Results And Discussion

4.1 Test Life

4.1.1 Sample Identification

The following convention in Table 4-1 is used for specimen identification in the graphs and charts in the results section. The numbers ranging from 1 to 42 are the sample numbers for data presentation. Each sample number corresponds to an FRP configuration, whose nomenclature was explained in the procedures section 3.2.3.2.

Table 4-1 Sample Identification

Sample Identification			
1	LW Control 1	22	NW Control 1
2	LW Control 2	23	NW Control 2
3	LW Control 3	24	NW Control 3
4	LW - G- F- 1L - 1	25	NW - G - F- 1L - 1
5	LW - G - F- 1L - 2	26	NW - G - F- 1L - 2
6	LW - G - F- 1L - 3	27	NW - G - F- 1L - 3
7	LW - G - F- 2L - 1	28	NW - G - F- 2L - 1
8	LW - G - F- 2L- 2	29	NW - G - F- 2L - 2
9	LW - G - F- 2L - 3	30	NW - G - F- 2L - 3
10	LW - C - F- 1L - 1	31	NW - C - F- 1L - 1
11	LW - C - F- 1L - 2	32	NW - C - F- 1L - 2
12	LW - C - F- 1L - 3	33	NW - C - F- 1L - 3
13	LW - C - F- 2L - 1	34	NW - C - F- 2L - 1
14	LW - C - F- 2L - 2	35	NW - C - F- 2L - 2
15	LW - C - F- 2L - 3	36	NW - C - F- 2L - 3
16	LW - C -S- 1L - 1	37	NW - C - S- 1L - 1
17	LW - C - S- 1L - 2	38	NW - C - S- 1L - 2
18	LW - C - S- 1L - 3	39	NW - C - S- 1L - 3
19	LW - C - S- 2L - 1	40	NW - C - S- 2L - 1
20	LW - C - S- 2L - 2	41	NW - C - S- 2L - 2
21	LW - C - S- 2L - 2	42	NW - C - S- 2L - 3

4.1.2 Length of time until sample removal (Test Life)

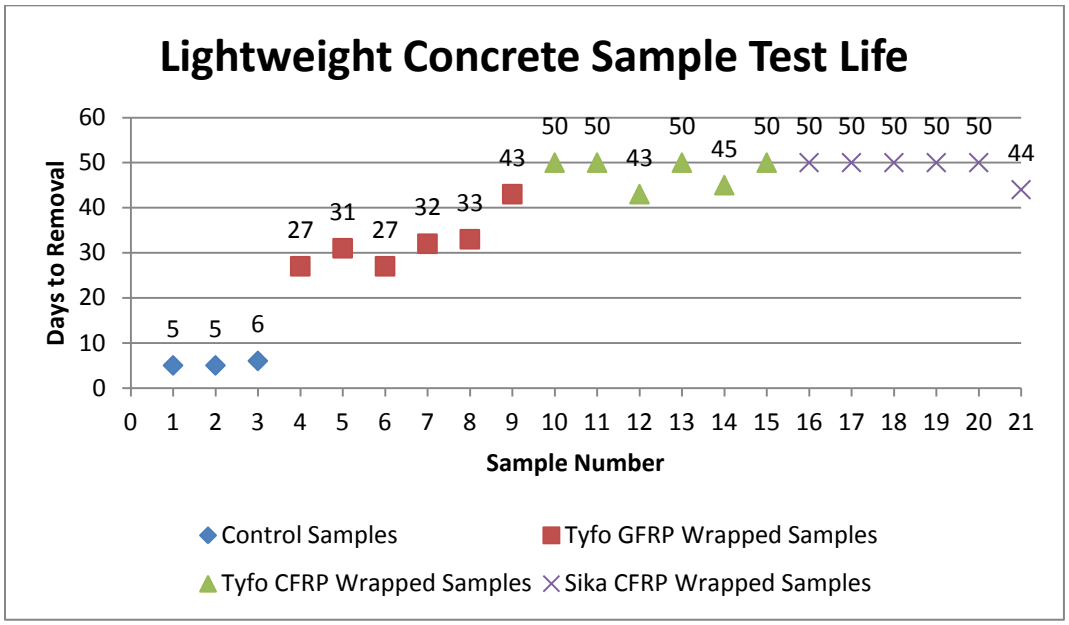

Figure 4-1 Lightweight Concrete Sample Test Life

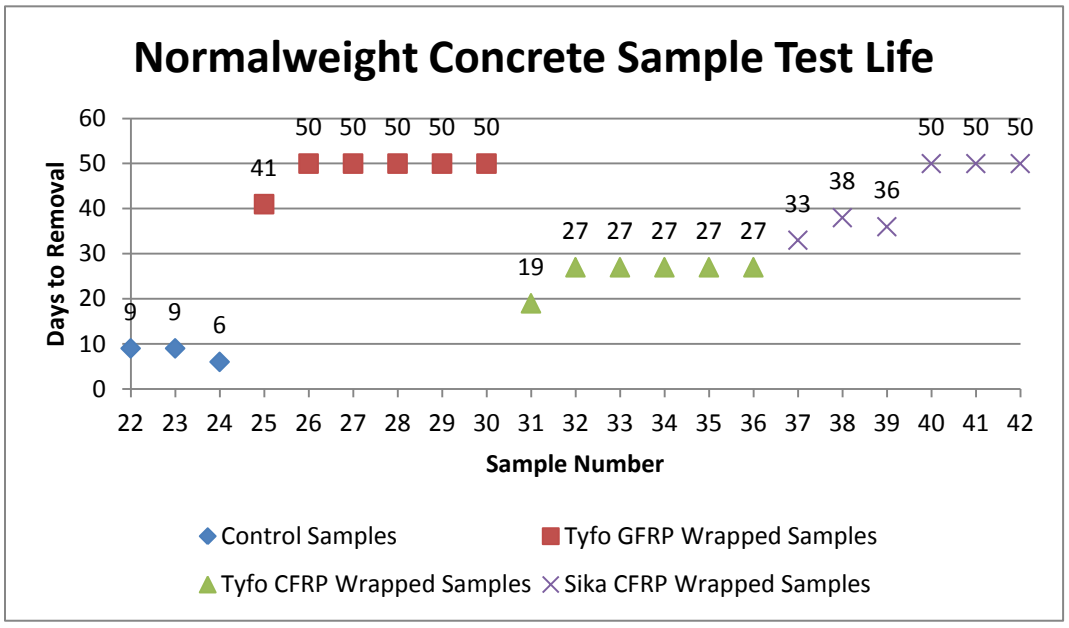

Figure 4-2 Normalweight Concrete Sample Test Life

4.1.2.1 Wrapped Lightweight Concrete vs. Control Samples

Table 4- 2 Test Life for Wrapped Lightweight Concrete Specimens

	Average Test Life (Days)	Test Life Increase (%)
LW Control	5.33	
LW - G -F -1L	28.33	531.25
LW - G - F - 2L	36.00	675.00
LW - C - F -1L	47.67	893.75
LW - C - F - 2L	48.33	906.25
LW -C - S - 1L	50.00	937.50
LW - C - S -2L	48.00	900.00

The table above shows the average test life were left in the tank, as well as the percentage of test life increase due to the FRP wrap. Test life was defined as the amount of time that the samples were immersed in the tank, which ended when samples were removed due to specimen failures or the test ended after 50 days. Failure modes will be discussed in section 4.1.3. Samples with FRP wrap had a minimum of five times as long of test life as the control specimens. The greatest increase was shown to be the lightweight concrete wrapped with one layer of Sika FRP with SikaDur epoxy, however this is misleading because of an FRP rupture in one of the samples of the Sika FRP with two layers. In all other tests, the Sika wrapped FRP with two layers outperforms the one layer, so this is more of an anomalous result. The lightweight concrete clearly performed better with CFRP than it did with GFRP, regardless if one or two layers was used. This is somewhat surprising in that the type of fiber is usually not what controls the corrosion, but rather the type of epoxy. It is possible that the GFRP layers suffered from some degradation while immersed in the salt solution. This effect has been seen in other research, and will be examined in more detail in the discussion section. Aside from one sample that ruptured, the lightweight concrete benefited slightly when using two layers of FRP as opposed to one.

4.1.2.2 Wrapped Normalweight Concrete vs. Control Samples

Table 4- 3 Test Life of Wrapped Normalweight Concrete Specimens

	Average Test Life (Days)	Test Life Increase (%)
NW Control	8.00	
NW - G -F -1L	47.00	587.50
NW - G - F - 2L	50.00	625.00
NW - C - F -1L	24.33	304.17
NW - C - F - 2L	27.00	337.50
NW -C - S - 1L	35.67	445.83
NW - C - S -2L	50.00	625.00

The normalweight concrete, in general, demonstrated greater test life when wrapped with the GFRP than with the CFRP. Part of this is due to a peculiar form of failure that the normalweight concrete seemed to suffer when wrapped with the TCH-41 system. The specimens corroded at the interface between the concrete and the rebar at a much faster rate than the rest of the specimens, therefore the specimens had to be removed from the tank despite the fact that they had not failed in a more conventional manner, such as in cracking of the concrete. This failure will be detailed more in the next section. The samples wrapped with Sika FRP performed much better in terms of specimen life when two wraps were used as opposed to one wrap. The test life increased a minimum of nearly four times of those of the control samples.

4.1.2.3 Lightweight Concrete vs. Normalweight Concrete

Table 4-4 Lightweight vs. Normalweight Concrete

	Average Test Life (Days)		
	LW	NW	% Difference
LW/NW Control	5.33	8.00	66.67
LW/NW - G -F -1L	28.33	47.00	60.28
LW/NW - G - F - 2L	36.00	50.00	72.00
LW/NW - C - F -1L	47.67	24.33	195.89
LW/NW- C - F - 2L	48.33	27.00	179.01
LW/NW-C - S - 1L	50.00	35.67	140.19
LW/NW - C - S -2L	48.00	50.00	96.00

The table above shows the difference between the length of test life in days for lightweight and normalweight concrete with FRP wraps. The percent difference data shows how much test life the lightweight concrete has to normalweight concrete, so a number greater than 100% means that the lightweight concrete had longer test life, and a number less than 100% means the normalweight concrete had longer test life. The normalweight concrete performed better than lightweight with GFRP wraps, whereas the lightweight concrete performed better with CFRP wraps in general. The normalweight concrete by itself lasted longer than the lightweight concrete, which is expected due to the fact that lightweight concrete is very porous. However, as explained in the literature review section, lightweight concrete benefits from several time dependent enhancements. These include an enhanced transition zone between the cement matrix and aggregate, similar elastic properties between the cement and aggregates, internal curing, and pozzolanic reactions. More detailed explanations of these are found in the literature review. The FRP may have been able to form a barrier around the concrete to reduce and delay the ingress of chlorides, allowing the lightweight concrete time to be able to benefit from these enhancements.

4.1.3 Types of Sample Failures

Table 4-5 Concrete Sample Failures

Concrete Sample Failures			
1	C	22	C
2	C	23	C
3	C	24	C
4	C	25	C
5	C	26	E
6	C	27	E
7	C	28	E
8	C	29	E
9	C	30	E
10	E	31	C
11	E	32	L
12	D	33	L
13	E	34	L
14	D	35	L
15	E	36	L
16	E	37	C
17	E	38	C
18	E	39	C
19	E	40	E
20	E	41	E
21	R	42	E

As mentioned before, there were three expected types of failures observed in this experiment: concrete cracking accompanied by a raise in current, delamination of the outermost layer of FRP, and FRP rupture. The concrete cracking is a form of failure in the concrete itself, indicating a loss of service life to the concrete. The other failures are FRP failures, which doesn't necessarily indicate that the concrete can no longer function, but it does reduce the effectiveness of the FRP. Aside from these, another unexpected

form of failure occurred due to an excessive localized current. These types of failures are detailed below.

4.1.3.1 Cracking in concrete substrate

The majority of the failures occurred due to the concrete cracking from the pressure caused by the corrosive products that were formed. The cracking was observed at the top of the specimen, beginning near the rebar and propagating towards the sides. The samples were removed when visible cracking appeared and had reached the sides of the cylinders. Seventeen of the samples had this type of failure.

Figure 4-3 Concrete Cracking

4.1.3.2 Delamination of the FRP from the Substrate

When an insufficient bond between the FRP and substrate is present, the FRP will delaminate, or peel away from the substrate. The presence of voids or irregularities in the concrete surface during the initial installation of the FRP can cause this problem. The epoxy itself can also fail while the FRP is in use. In real structures an FRP delamination can cause a reduction in the strength and stiffness enhancements that the

FRP provides, so it does not indicate a loss of service life in the concrete itself, however the FRP would likely have to be reapplied. When a delamination failure was found the sample was removed from the tank. This form of failure was found in two of the samples. Figure 4-4 shows a delaminated sample. Both of the samples that failed from this were delaminated towards the bottom of the cylinder, where the FRP peeled away from the substrate. When these samples were removed from the tank, water poured from where it was trapped between the wrap and the concrete. This indicated that the sample had delaminated. Approximately 15-20% of the FRP was estimated to have delaminated from the concrete.

Figure 4-4 Debonding of the FRP from the substrate

4.1.3.3 FRP Rupture

Sample 21, a lightweight concrete with two layers of Sika Wrap, had this form of failure. The FRP ruptured towards the bottom of the sample, which allowed the solution

to enter the area between the first layer and second layer of FRP. Due to the presence of the second FRP layer and the epoxy there was still very little corrosive damage, but like the samples that failed from delamination the FRP would most likely have to be removed and reapplied to the sample. Therefore, the sample that showed this sign of failure was removed from the tank.

Figure 4-5 FRP rupture in Sample 21

4.1.3.4 Excessive Localized Current

Normalweight samples 32-36 all showed a peculiar form of failure, in which the rebar at the concrete-rebar interfaced contained an excessive localized mass loss at the interface between the concrete and the rebar. Spainhour et.al. (2003) encountered the same form of failure during their experiments. These samples showed an extreme form of localized corrosion versus other samples, which had more uniform corrosion throughout the rebar. During the test a very condensed form of dark corrosion would appear on the surface of the cylinder at the concrete-rebar interface. Although the

concrete samples had not cracked and still had service life, the localized corrosion created difficulties in corroding the wire itself. In addition, the localized corrosion created mass loss in the rebar that, if continued, would have caused the portion of the rebar extending out of the concrete to be corroded off from the rest of the rebar, making it impossible to continue the accelerated corrosion on the samples.

According to Spainhour et. al. (2003), the localized corrosion is a product of the confinement effect of the FRP, which restrains the expansion of concrete. This type of failure is not seen in actual concrete structures due to the fact that the entire rebar is generally completely embedded in the concrete. It was theorized that since the corrosive products could not expand and cause tensile cracks, they instead compacted around the reinforcement. As corrosive products kept being formed, they were forced to leave the system around the interface, in the form of a dark green or black paste This localized corrosion can be seen in Figures 4-6 and 4-7. It is interesting to note that this form of failure was only seen in normalweight concrete samples. It is possible that this failure may have developed in the lightweight concrete had they remained in the tank for a longer period of time than the 50 test day period, however it has been seen in some research that confinement effects are less for lightweight concrete than they are for normalweight, which may indicate why this was not seen for the lightweight samples. This will be explained in more detail in the discussion section.

Figure 4-6 Localized Corrosion at the Concrete-Rebar Interface

Figure 4-7 Rebar subjected to extreme localized corrosion

4.1.3.5 End of the test

Seventeen samples lasted until the end of the test. Nine of these were lightweight and eight were normalweight concrete. Many of these samples showed little

to no signs of corrosion in the form of rusting, and the FRP appeared to have achieved a very strong bond with the concrete. These samples were observed to have been much tougher to break when extracting the rebar than the samples that had been cracked.

4.2 Chloride Content

Chloride content was used as a relative measure to indicate the ability of the FRP systems to provide a barrier to chloride ingress. The equation specified by ASTM C1152 to find the chloride content is as follows:

$$Cl, \% = \frac{3.545[(V1 - V2)N]}{W}$$

where,

V_1 = milliliters of 0.05 N $AgNO_3$ solution for sample titration (equivalence point)

V_2= milliliters of 0.05 N $AgNO_3$ solution for blank titration (equivalence point)

N = exact normality of 0.05 $AgNO_3$ solution

W = mass of sample, g

Because this is not a referee analysis, the blank titration can be omitted, so V_2 is equal to zero.

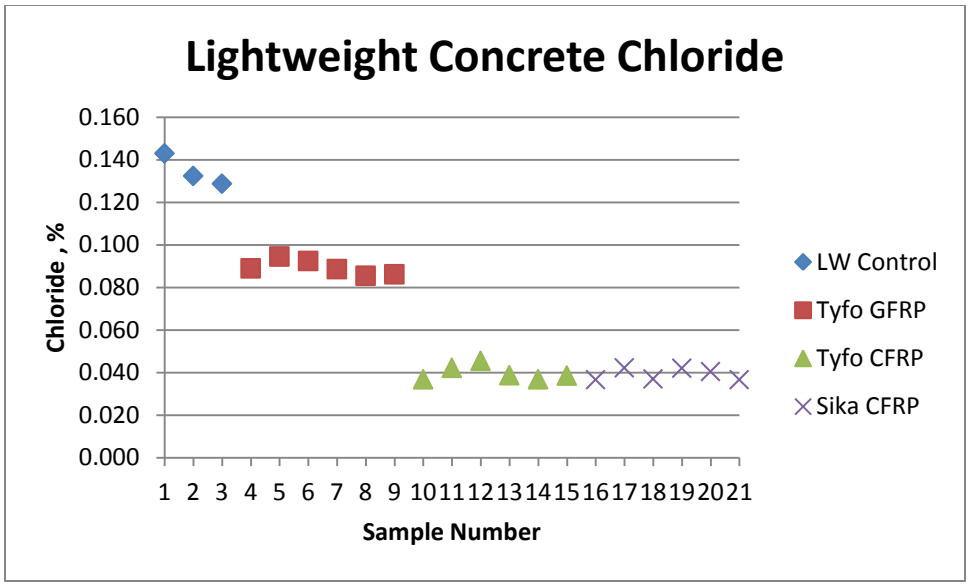

Figure 4-8 Percent Chloride in Lightweight Concrete Samples

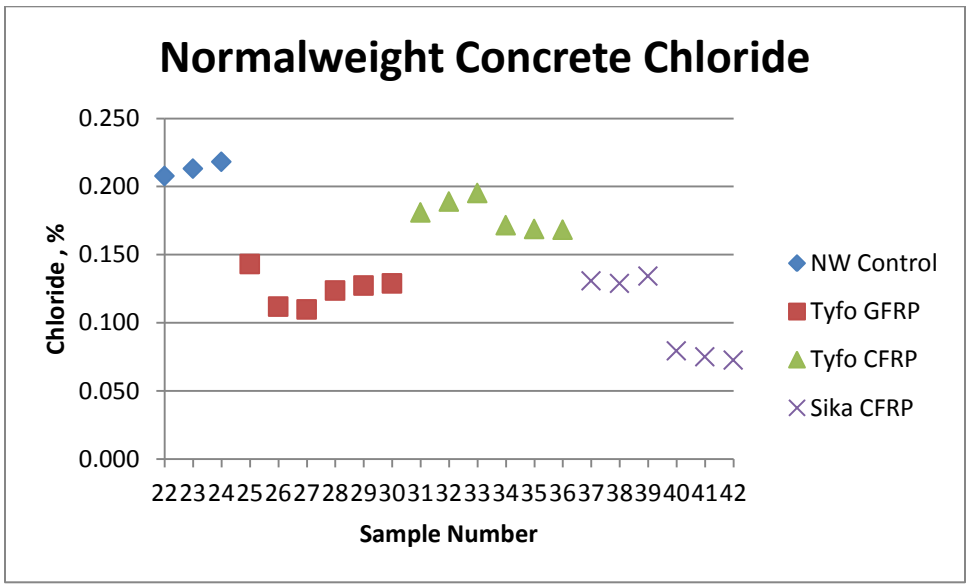

Figure 4-9 Percent Chloride in Normalweight Concrete Samples

Figures 4-8 and 4-9 show the chloride content for lightweight and normalweight samples, respectively. Due to the acid-soluble aggregates in the normalweight concrete, the chloride percentages are higher than for the lightweight. Both the lightweight and normalweight showed the lowest amount of acid soluble chloride for the 2 layer Sika CFRP configuration. The chloride content was highest in the control sample for the lightweight concrete samples and normalweight concrete samples. All of the samples showed less chloride content when wrapped versus unwrapped. For the lightweight concrete, the Sika CFRP with 2 wraps had 3.5 times less chloride content than the control samples, and about 2 times less chloride content than the Tyfo GFRP. For the normalweight concrete, the Sika CFRP with 2 wraps had nearly 4 times less chloride content than the control samples. The Sika CFRP with one layer of wrap performed about the same as the Tyfo GFRP. It is also seen from the chloride content data that there was not much difference between one and two layers for the lightweight concrete. In contrast, there was a discernible difference between one and two layers for normalweight concrete. This corresponds with other data that normalweight concrete may benefit more from multiple layers of wrap than lightweight concrete.

4.3 Rebar Mass Loss

Table 4-6 Rebar Weights Before the Test Begins

Rebar Weights- Before Test (grams)										
1	**2**	**3**	**4**	**5**	**6**	**7**	**8**	**9**	**10**	**11**
96.11	98.23	94.52	98.06	97.23	98.14	97.15	95.33	97.54	98.22	96.14
12	**13**	**14**	**15**	**16**	**17**	**18**	**19**	**20**	**21**	**22**
96.53	97.24	96.26	96.04	97.13	96.54	94.24	96.35	97.13	96.54	96.56
23	**24**	**25**	**26**	**27**	**28**	**29**	**30**	**31**	**32**	**33**
99.22	98.9	96.12	98.51	98.57	95.55	96.52	96.5	97.5	96.22	96.41
34	**35**	**36**	**37**	**38**	**39**	**40**	**41**	**42**		
97.08	96.33	97.21	95.12	96.24	95.5	95.51	97.24	96.51		

Table 4-7 Rebar Weights After Accelerated Corrosion

Rebar Weights- After Corrosion (grams)										
1	**2**	**3**	**4**	**5**	**6**	**7**	**8**	**9**	**10**	**11**
80.33	81	79.8	88.45	86.3	90.2	90.22	86.77	91.2	97.2	95.26
12	**13**	**14**	**15**	**16**	**17**	**18**	**19**	**20**	**21**	**22**
94.90	96.35	95.4	94.3	96.12	95.59	92.96	94.55	96	95.26	83.91
23	**24**	**25**	**26**	**27**	**28**	**29**	**30**	**31**	**32**	**33**
84.65	85.52	89.2	94.88	92.97	91.2	91.47	92.31	83.65	76.77	75.43
34	**35**	**36**	**37**	**38**	**39**	**40**	**41**	**42**		
78.5	81.45	81.91	89.2	89.7	90.07	95.03	96.41	96.33		

Table 4-8 Percentage of Rebar Mass Loss

Rebar Weights- Mass Loss (%)										
1	**2**	**3**	**4**	**5**	**6**	**7**	**8**	**9**	**10**	**11**
16.42	17.54	15.57	9.80	11.24	8.09	7.13	8.98	6.50	1.04	0.92
12	**13**	**14**	**15**	**16**	**17**	**18**	**19**	**20**	**21**	**22**
1.69	0.92	0.89	1.81	1.04	0.98	1.36	1.87	1.16	1.33	13.10
23	**24**	**25**	**26**	**27**	**28**	**29**	**30**	**31**	**32**	**33**
14.68	13.53	7.20	3.68	5.68	4.55	5.23	4.34	14.21	20.21	21.76
34	**35**	**36**	**37**	**38**	**39**	**40**	**41**	**42**		
19.14	15.45	15.74	6.22	6.80	5.69	0.50	0.85	0.19		

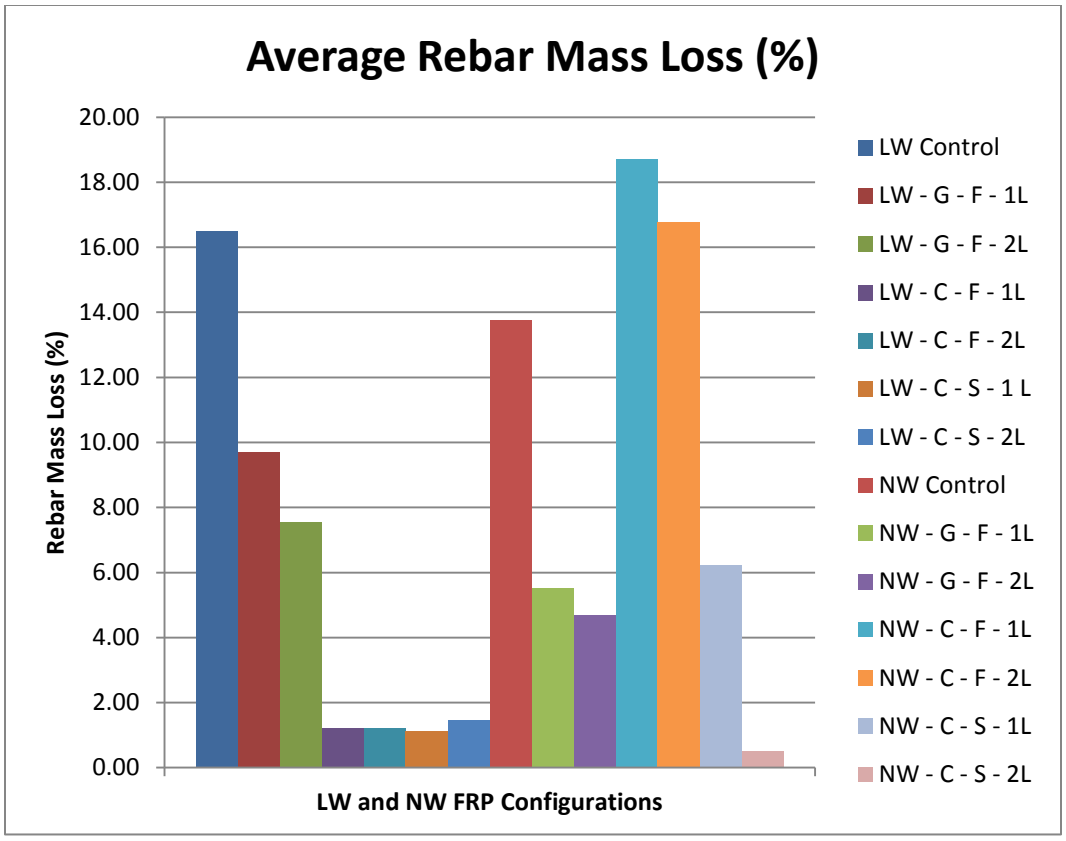

Figure 4-10 Average Rebar Mass Loss

The tables above show the rebar weights before the accelerated corrosion starts, after the test has ended, and the percentage of mass loss. Figure 4-10 gives a graphic representation of the average rebar mass loss for each different FRP configuration. With the exception of the rebars that failed due to an excessive localized current, all the other rebars demonstrated a decrease in the percentage of mass loss when compared to the control samples.. The mass loss percentage correlates well with the specimen test life, where the specimens that lasted longer had a lesser percentage of total mass loss. This suggests that the samples with longer test life had a lower corrosion rate, as the corrosion in this experiment is not linear with time. Once the concrete develops cracks

the chlorides flow to the rebar and create a current flow that exacerbates the corrosion. The FRP helps provide a barrier to reduce the number of these chlorides that can reach the rebar, whereas the control samples have no barrier to the ingress of chlorides, so once they crack the corrosion in the samples escalate rapidly.

As mentioned previously, samples 32-36 had an excessive localized current which corroded the rebar at the concrete interface. This localized corrosion created extensive mass loss in one location, due to the leached corrosive product that was forced through the interface. This mass loss is greater than that of the control samples, indicating that without the confinement it is likely these samples would have cracked, rather than the corrosion leaching at the concrete-rebar interface. This shows the effect confinement can have in assisting in corrosion protection and increasing concrete life, so although the epoxy type is the greatest factor in resisting corrosion, the wrap can become a factor once corrosion has initiated and corrosion products are beginning to form.

The effects of using one or two wraps appeared to have more pronounced effects in the normalweight concrete than it did for the lightweight concrete, which was also seen in the chloride content data. The mass loss for the normalweight concrete with one layer of Sika CFRP was much higher than it was for two layers. The lightweight concrete, however, appeared to be more consistent whether one or two layers were used. This may indicate that the effects of the confinement for using multiple layers are more pronounced for normalweight concrete than they are for lightweight concrete.

Samples 2, 7, 8, and 34 had different concrete clear covers than the standard 1/2", as mentioned before. Sample 2, with a 1/4" cover, had a slightly greater mass loss at 17.54% than samples 1 and 3 at 16.42% and 15.57%, respectively. Sample 7 with a 3/4" cover had a greater mass loss than sample 9, which had 1/2" cover, but less than sample 8, which had 1/4" cover. Sample 34 had a 3/4" cover, yet had greater mass loss

than samples 35 and 36, which had 1/2" cover. Sample 34 failed by localized corrosion current, which is not a form of failure found in the field, so it is not appropriate to draw conclusions of cover based on that sample. The other samples indicate that concrete clear cover had some impact on the mass loss of samples, yet the values were still close to other similar samples. The samples with 1/4" cover appeared to experience slightly more mass loss than the 1/2" samples, while there did not appear to be a noticeable difference between the bars with 1/2" cover and 3/4" cover, although this was a small sample size.

4.4 Current Measurements

The current measurements were taken for the worst case for each FRP configuration. These measurements are correlated with the actual mass loss and the theoretical mass loss using Faraday's Law. The equation for Faraday's Law is (Maaddawy and Soudki, 2003):

$$\Delta M = \frac{I * t * Aw}{n * F}$$

where M = mass of metal dissolved or converted to oxide, grams

I = current, Amps

t = time, seconds

A_w = atomic weight (56 for iron)

n = valency (2)

F = Faraday's constant (96,500 coulombs/equivalent mass)

According to Maaddawy and Soudki, Faraday's Law should be able to accurately predict metal loss up to approximately 7.5%, then as the loss of steel gets higher , Faraday's Law tends to overestimate the amount of metal loss.

Table 4-9 Lightweight Concrete Current Measurement and Mass Loss

	Current (Amps)	Time (s)	Mass Loss (g)	Predicted Mass Loss (g)	% Diff
LW Control -2	0.18	432000	17.23	22.56	23.63
LW - G -F -1L - 2	0.017	2678400	10.93	13.21	17.27
LW-G-F-2 - 2	0.0121	2851200	8.56	10.01	14.49
LW-C-F-1 - 3	0.0017	3628800	1.63	1.79	8.94
LW-C-F-2 - 3	0.0014	4320000	1.71	1.75	2.56
LW-C-S-1-3	0.00105	4320000	1.28	1.32	2.75
LW-C-S-2-1	0.0017	3801600	1.8	1.88	4.01

Table 4-10 Normalweight Concrete Current Measurement and Mass Loss

	Current (Amps)	Time (s)	Mass Loss (g)	Predicted Mass Loss (g)	% Diff
NW Control -2	0.078	777600	14.57	17.60	17.21
NW - G -F -1L - 2	0.0058	4320000	6.92	7.27	4.82
NW-G-F-2 - 2	0.0042	4320000	5.05	5.26	4.08
NW-C-F-1 - 3	0.038	2332800	20.98	25.72	18.43
NW-C-F-2 - 3	0.0262	2332800	14.88	17.73	16.09
NW-C-S-1-3	0.0072	3283200	6.54	6.86	4.65
NW-C-S-2-1	0.00068	4320000	0.83	0.85	2.62

The two tables above show the measured current at the time when the sample was removed from the tank, the mass loss, predicted mass loss, and percent difference between theoretical and actual mass loss. For the rebars that had high mass losses, the predicted mass loss according to Faraday's Law overestimated the actual mass losses as much as 23.63%. For lower mass losses, Faraday's Law had greater accuracy in predicting results.

The currents shown correspond well with the other data. The control samples contained the highest currents, and the 2 wrap Sika CFRP had extremely low current values. This correlates well with the sample life data, where the control samples had several visible cracks and the Sika wrapped samples showed almost no signs of corrosion whatsoever. This indicates that the Sika epoxy created a very strong barrier to

the salt solution, allowing very little paths to the rebar for chloride ions to penetrate and create a path for current flow.

4.5 Discussion

After reviewing the data, it is evident that using FRP wraps can provide significant corrosion protection to concrete, whether it is lightweight or normalweight. The epoxy creates a barrier to prevent chloride ions to penetrate the concrete, and the FRP wraps allow confinement of the samples to restrict expansion of the concrete, which can delay the onset of spalling. The data seemed to suggest that CFRP wraps were more effective in lightweight concrete, whereas the GFRP wraps performed better for the normalweight concrete. There is still insufficient data to determine the exact reasons for this, but some theories can be presented based on the properties of the two different types of concrete.

As mentioned in section 2.1.3 of the literature review, there have been several studies that have noted that the permeability of lightweight concrete can be lower than that of normalweight concrete. These have been attributed to the elastic compatibility between lightweight aggregates and cement, reducing differential stresses that can occur between two materials of different stiffnesses; pozzolanic reactions from the lightweight aggregate that improve the interface of the lightweight aggregate and cement matrix through chemical reaction interlocking; and the reduction of internal bleeding that may occur through a hygrol equilibrium that occurs through the availability of water in the lightweight aggregate. Another important factor that has been cited in studies as improving permeability is internal curing, which is the process of releasing stored water from the lightweight aggregates to the surrounding cement to continue hydration of the cement while the concrete is in service. These benefits are explained in greater detail in the literature review section. A very important point to note is that many of these

enhanced properties are time dependent. For instance, a long term extension in curing due to internal curing can develop a reduction in permeability (ACI Committee 213, 2003). The results in this research indicated that the control lightweight concrete failed before the normalweight concrete, which means it can be deduced that the lightweight control concrete was more permeable than the normalweight control concrete at an early age. The concrete wrapped with FRP, however, may have been effective in providing an early barrier to chloride ingress, allowing the lightweight concrete an opportunity to benefit from the time-dependent effects noted above. This may be a reason why the lightweight concrete tended to perform better with the CFRP than the normalweight concrete.

As noted before, the GFRP did not perform as well as the CFRP for the lightweight concrete. One possible reason may have been due to deterioration in the GFRP sheets from the salt water solution. Gharachorlou and Ramezanianpour (2010) noted differences in the performance of GFRP and CFRP wrapped beams when exposed to an accelerated corrosion test, where the CFRP beams performed better in terms of . They noted this effect was likely due to the degradation of glass fibers that were continually immersed, as glass fibers can be damaged from continuous immersion in moisture, whereas carbon fibers are not susceptible to this. Salt solutions are known to cause attack on glass composites by leaching alkali from the glass fiber (GangaRao et. al., 2006). This may have reduced the effectiveness of the GFRP wrapped lightweight concrete cylinders in this experiment and caused them to fail earlier than the CFRP wrapped specimens. However, this was not the case for the normalweight concrete, which tended to perform better with GFRP wrapping versus CFRP wrapping. Thus, there may have been some incompatibility with the specific GFRP used and the specific lightweight concrete used. As noted before, the GFRP fibers and epoxy were not new

materials, so they may have lost some properties that could help provide greater corrosion protection to the lightweight concrete. More research utilizing different manufacturer materials is necessary to verify the compatibility between GFRP and lightweight concrete as it pertains to corrosion.

Another aspect that is unclear is the absorption of epoxy into the lightweight aggregate particles themselves. It is likely that some epoxy was absorbed into the aggregate, however whether this absorption was limited to mostly surface aggregates or aggregates throughout the concrete is not readily apparent. How the absorption affects the bond between the concrete substrate and the FRP is a point for future research. The absorption of the epoxy into the aggregates could potentially lead to less epoxy being available for bond between the FRP and concrete substrate, leading to a reduction in bond. This may explain why some debonding failures were found in some of the lightweight concrete samples in the experiment. Some epoxy manufactures have recommended the application of more than one coat of epoxy for porous substrates such as lightweight concrete (ChemCo Systems). The bond for lightweight concrete with FRP should be examined in greater detail.

The effects of using multiple layers of FRP for the lightweight concrete did not appear to be as pronounced for the lightweight concrete as they were for the normalweight concrete samples, in terms of bar mass loss or chloride ingress. The use of multiple layers generally provides more confinement to the concrete, which assists in resisting the cracks that occur from the corrosion products. Other research has indicated that the effects of confinement are not as pronounced for lightweight concrete as they are for normalweight concrete (Axson, 2008; Shah et. al., 1983; Fu et. al., 2011). It is possible for this study that the confining effects of the use of multiple layers of FRP may not have been realized as well as they were for the normalweight concrete. This could

mean that for lightweight concrete, there is a greater reduction in permeability due to the improved aggregate cement matrix mentioned earlier, however, when corrosion is initiated, it may take longer for the normalweight concrete to crack due to better confining effects. It should also be mentioned that several of the lightweight concrete samples had yet to fail for the CFRP samples. It is possible that had they been allowed to corrode until cracking, the benefits of confinement could be more easily seen. For future research, longer periods of corrosion time until cracking should be examined to determine if there are differences in the time to initiation of corrosion until cracking for lightweight concrete wrapped with CFRP.

It is important to note that the discussion here is mostly theoretical based on observations from the experiment and available literature. Much more research is needed to determine the validity of these points and to more accurately ascertain the capabilities of lightweight concrete with externally bonded FRP wraps. Due to the variable nature of lightweight aggregates and lightweight concrete, different effects may be observed than the ones that were found in this experiment. The lack of available literature on lightweight concrete and FRP in terms of corrosion protection means that more research is necessary to determine the terms of the behavior of FRP and lightweight concrete. Nevertheless, this experiment did demonstrate that FRPs can be beneficial for both types of concrete for protection against corrosion.

Chapter 5

Conclusion And Recommendations

The research presented herein attempted to examine the effects of FRP in terms of corrosion protection afforded to lightweight concrete. The following conclusions were found from this research:

- Both lightweight concrete and normalweight concrete demonstrated increased length of test life, lower chloride content, and lower rebar mass loss when wrapped with FRP versus unwrapped samples
- Lightweight concrete wrapped with CFRP demonstrated longer test life overall than CFRP wrapped normalweight concrete, whereas normalweight concrete wrapped with GFRP demonstrated longer test life than GFRP wrapped lightweight concrete. Previous research on the permeability of lightweight concrete has indicated that lightweight concrete benefits from several time dependent improvements that reduce its permeability to levels equal to or lower than normalweight concrete. These include better elastic compatibility between lightweight aggregates and cement, improved hydration of cement from internal curing, pozzolanic reactions from the lightweight aggregates that improve the quality of the concrete, and reduction of internal bleeding. The FRP wraps may have provided an early barrier to the ingress of chlorides, allowing the lightweight concrete to realize some of these improvements over time.
- Mass loss appeared to correlate well with test life and chloride content. Wrapped specimens had less mass loss than the control samples, with the exception of the normalweight concrete samples wrapped with Tyfo

CFRP. These samples showed localized corrosion, likely occurring due to confinement from the CFRP wraps.

- It was observed that the use of multiple layers of wrap had more apparent effects in reduction in mass loss and chloride content for normalweight concrete than for lightweight concrete. Based on this and the previous conclusion points, it may indicate that the lightweight concrete had reduced permeability versus the normalweight concrete, whereas the normalweight concrete may have benefitted more from confinement effects.

Based on the results of this research, the following future research is recommended:

- Investigation of the absorption of epoxy in lightweight concrete. This may include testing the bond between the concrete substrate and the FRP to determine if the excess water in the lightweight aggregates affects the bond.
- The effects of confinement as it relates to corrosion should be further investigated, particularly in the differences between lightweight concrete and normalweight concrete.
- Larger specimens than the ones used in this research should be investigated. Longer periods of corrosion with conditions closer related to the field should be used in order to more accurately gauge corrosion effects.
- Investigating lightweight specimens that have already been corroded and repaired with FRP can be examined to gauge the effects of FRP after post repair.

- The concretes used in this study contained no admixtures of any kind. Mineral admixtures such as fly ash and silica fume are often used in construction in corrosive environments to increase strength and provide increased durability. The combined effects of admixtures and FRP should be looked at to provide a more accurate determination of field conditions.
- This study only used one type of lightweight aggregate, an expanded shale from ESCSI. Other lightweight aggregates should be studied due to their different properties, including absorption. These aggregates may demonstrate different effect than the ones utilized in this study. FRP materials from other manufacturers should also be tested.

Appendix A

Concrete Properties

Table A-1 Concrete Mix Amounts

Concrete Mixes (Units in Lbs. , Mixes for 1 yd^3)		
	Lightweight Concrete	**Normalweight Concrete**
Water	310	310
Cement (Type I/II)	700	700
Fly Ash (Class C)	0	0
Silica Fume	0	0
3/4" Limestone	0	1600
3/4" Streetman Lightweight Aggregate	900	0
Concrete Sand	1346	1321

Concrete Fresh Density Calculations - ASTM C138/138M - 10b

$$D = \frac{(M_c - M_m)}{V}$$

where

M_c = Mass of measure filled with concrete, lb or kg

M_m = Mass of measure, lb or kg

V = volume of measure, ft^3 or m^3

D = density, lb/ft^3

For measure used, dimensions were 8" diameter and 8.5" height

$$V = \pi * (4\ in)^2 * 8.5\ in = 427.26\ in^3 * \frac{1\ ft^3}{1728\ in^3} = 0.247\ ft^3$$

$$D = (43.88\ lb - 8.2\ lb) = \frac{35.68\ lb}{0.247\ ft^3} = 144.45\ \frac{lb}{ft^3}\ for\ normalweight\ concrete$$

$$D = (38.04\ lb - 8.2\ lb) = \frac{30.02\ lb}{0.247\ ft^3} = 121.54\ \frac{lb}{ft^3}\ for\ lightweight\ concrete$$

Lightweight Concrete Equilibrium Density Calculations - ASTM C567 - 05a

$$Oc = \frac{(M_{df} + M_{dc} + 1.2 * M_{ct})}{V}$$

where

O_c = calculated oven dry density, kg/m^3 (lb/ft^3)

M_{df} = mass of dry fine aggregate in batch, kg (lb)

M_{dc} = mass of dry coarse aggregate in batch, kg (lb)

M_{ct} = mass of cement in batch, kg (lb)

V = volume of concrete produced by batch, m^3 (ft^3)

$$V = \frac{M}{D}$$

where

M = total mass of all materials batched, lb or kg

$$V = \frac{(7 + 16 + 21 + 31)lb}{121.54\ \frac{lb}{ft^3}} = 0.617 ft^3\ for\ lightweight\ concrete$$

$$Oc\ = \frac{(31 +\ 20 + 1.2 * 16)lb}{0.617 ft^3} = 113.77 \frac{lb}{ft^3}$$

$$Ec\ =\ O_c + 3\ \frac{lb}{ft^3} = 116.77 \frac{lb}{ft^3}$$

where E_c = Calculated equilibrium density, lb/ft^3

Concrete cylinder strengths

Table A-2 Compressive Strengths

Specimen	1	2	3	Avg
LW	3960	3650	3850	3820
NW	3940	4450	4210	4200

Appendix B

ASTM C1152 Example Calculation

Normalweight 23

$$Cl, \% = \frac{3.545[(V1 - V2)N]}{W}$$

where,

V_1 = milliliters of 0.05 N $AgNO_3$ solution for sample titration (equivalence point)

V_2= milliliters of 0.05 N $AgNO_3$ solution for blank titration (equivalence point)

N = exact normality of 0.05 $AgNO_3$ solution

W = mass of sample, g

For normalweight 23,

W = 10.2 g

Millivolt reading for electrode submerged in water only

412 mV

Amount of silver chloride to get the reading to approximately 60 mV below water reading

V_1 = 12.2 mL

V_2 = 0 (not a referee analysis)

$$Cl, \% = \frac{3.545[(12.2\ mL - 0)0.05\ mol/L\ ]}{10.2\ g} = \mathbf{0.212}\ \%$$

References

ACI Committee 211, (1998), Standard Practice for Selecting Proportions for Structural Lightweight Concrete, ACI 211.2-98, American Concrete Institute.

ACI Committee 213, (2003), Guide for Structural Lightweight Aggregate Concrete, ACI 213R-03, American Concrete Institute.

ACI Committee 222R, (2001), Protection of Metals in Concrete against Corrosion,ACI 222R-01, American Concrete Institute.

ACI Committee 440R, (2007), Report on Fiber-Reinforced Polymer (FRP) Reinforcement for Concrete Structures, ACI 440R-07, American Concrete Institute.

ACI Committee 440, (2008), Guide for the Design and Construction of Externally Bonded FRP Systems for Strengthening Concrete Structures, ACI 440.2R-08, American Concrete Institute.

American Water Works Association. Ductile Iron Pipe and Fittings, 2nd ed. American Water Works Association, Denver, CO, pg. 166-169.

ASTM. (2011). Standard Test Method for Acid-Soluble Chloride in Mortar and Concrete,ASTM C1543, Philadelphia. pg. 645-648

ASTM. (2011). Standard Practice for Preparing, Cleaning, and Evaluating Corrosion Test Specimens, ASTM G1-03, Philadelphia. pg. 20-28.

ASTM. (2011). Standard Test Method for Determining Density of Structural Lightweight Concrete, ASTM C567-05a, Philadelphia. pg. 318-320.

ASTM. (2011). Standard Specification for Lightweight Aggregates for Structural Concrete, ASTM C330/300M-09, Philadelphia. pg. 318-320.

Axson, D. (2008). "Ultimate Bearing Strength of Post-tensioned Local Anchorage Zones in Lightweight Concrete," Master's Thesis, Virginia Polytech Institute and State University, Blacksburg

Berver, E., Jirsa, J., Fowler, D., Wheat, H. and Moon, T. (2001). “Effects of Wrapping Chloride Contaminated Concrete with Fiber Reinforced Plastics”. FHWA/TX-03/1774-2, Austin, TX.

Chandra, S and Berntsson, L. (2003). *Lightweight aggregate concrete: science, technology, and applications*. Nowrich, N.Y.: Noyes Publications/William Andrew Pub., c 2003. pg. 134-138.

http://chemcosystems.com/tech_bondingcon.html

Daily, Steven F. (2003). "Understanding corrosion and cathodic protection of reinforced concrete structures". Corrpro Companies, Incorporated, 2003.

Detwiler, R. J., Kjellsen, K. O., and Gjorv, O. E., (1991), ‘‘Resistance to chloride intrusion of concrete cured at different temperatures.’’ ACI Materials Hournal, Vol. 88, No. 1, pp. 19-24, 1991

Fu, Z., Ji, B., Lv, L., and Yang, M. (2011) The Mechanical Properties of Lightweight Aggregate Concrete Confined by Steel Tube. Design, Construction, Rehabilitation, and Maintenance of Bridges: pp. 33-39.

Gadve, S and Mukherjee, A. (2008). "Active Protection of Fiber Reinforced Polymer Wrapped Reinforced Concrete Structures Against Corrosion". Proquest Science Journals, Vol. 67, No. 2, pp. 1-11.

GangaRao, Hota V.S., Taly, Narendra, and Vijay, P.V. (2007). Reinforced Concrete Design With FRP Composites, Taylor & Francis Group, Boca Raton, FL, Durability: Aging of Composites, pg.53-54, 87.

Gharachorlou, A. and Akbar , A. (2009), "Resistance of concrete specimens strengthened with FRP sheets to the penetration of chloride ions", The Arabian J.for Sci and Engg., 35, Number 1B, pg. 141-154.

Heffington, J. A., 2000, "Development of High Performance Lightweight Concrete Mixes for Prestressed Bridge Girders," Master's Thesis, The University of Texas, Austin, May

Holm, T.A. (1980). "Performance of Structural Lightweight Concrete in a Marine Environment." International Symposium, St. Andrews-By-the-Sea, Canada, August 1980.

Holm, Thomas A. and Bremner, Theodore w. (2000). "State-of-the-Art Report on High-Strength, High-Durability Structural Low-Density Concrete for Applications in Severe Marine Environments." ERDC/SL TR-00-3, U.S. Army Engineer Research and Development Center, Vicksburg, MS.

http://www.fyfeco.com

Xuemei Liu , KokSeng Chia, Min-Hong Zhang (2010). "Development of lightweight concrete with high resistance to water and chloride-ion penetration." Cement and Concrete Composites, V. 32(I.10), November, pp.: 757-766.

Mackie, G. K., (1985) “Recent Uses of Structural Lightweight Concrete,” Concrete Construction, Vol. 30, No. 6 (Jun. 1985) pp. 497-502.

Masoud S, Soudki KA. (2006). "Evaluation of Corrosion Activity in FRP Repaired RC beams". Cem Concr Compos 2006;28:9 69–77

Murugesh, Ganapathy. (2008). “Lightweight Concrete and the New Benicia-Martinez Bridge.” Concrete Bridge Views. 49: 1-13. *HPCBridgeViews.*

Norton Corrosion Limited, "Fundamentals of Cathodic Protection," Norton Corrosion Limited, LLC, Woodinville, WA

Park, Si-Hwan; Robertson, Ian N,; and Riggs, Ronald H. (2002). "A Primer for FRP Strengthening of Structurally Deficient Bridges". University of Hawaii, College of Engineering. Research Report UHM/CE/02-03.

Protection Technology Group, "Dissimilar Metals May Take Away Your Protection," PolyPhaser, Hayden, ID, 1485-007, 2011.

S.P. Shah, A.E. Naaman, J. Moreno, (1983) " Effect of confinement on the ductility of lightweight concrete", International Journal of Cement Composites and Lightweight Concrete, Volume 5, Issue 1, February 1983, Pages 15-25, ISSN 0262-5075,

Sen, R. (2003), "Advances in the Application of FRP for Repairing Corrosion Damage", Progress in Structural Engineering and Materials, Vol. 5, No. 2, pp. 99-113.

Stanish KD, Hooton RD, Thomas MDA, (1997), "Testing the chloride penetration resistance of concrete: a literature review", FHWA contract DTFH61, Department of Civil Engineering, University of Toronto, Canada

Spainhour, Lisa K. and Yazdani, Nur. (2002). "Composite Fiber Wrapping for Protection, Strengthening, and Repair of Bridge Elements in the Splash Zone". National Science Foundation Report. Final Report: 9504193.

Spainhour, L. K., & Wootton, I. A. (2008). "Corrosion process and abatement in reinforced concrete wrapped by fiber reinforced polymer". *Cement and Concrete Composites*, *30(6)*, 535-543.

Suh, K., Mullins, G., Sen, R., and Winters, D. (2007). "Effectiveness of FRP in reducing corrosion in a marine environment." ACI Struct. J. 104, 76–83.

Tamer A, Maaddawy E, Soudki KA. (2003). "Effectiveness of impressed current technique to simulate corrosion of steel reinforcement in concrete," J Mater Civil Eng;15(1):41–7.

United States. National Cooperative Highway Research Program. Transportation Research Board of the National Academies. (2013). *High-Performance/High-Strength Lightweight Concrete for Bridge Girders and Decks.* (NCHRP Report 733*).*

usa.sika.com

Wall and Freeman. (2003). " Rapid Chloride Permeability of Structural Lightweight Aggregate Concrete Compared with Normal Density Concrete Having Similar Proportions." Carolina Stalite Company Research Lab, Gold Hill, North Carolina.

Wootton, I. A., Spainhour, L. K., & Yazdani, N. (2003). "Corrosion of steel reinforcement in carbon fiber-reinforced polymer wrapped concrete cylinders". *Journal of Composites for Construction*, *7(4)*, 339-347.

www.ESCSI.org

Biographical Information

Eric Goucher earned his Bachelor's of Science Degree in Civil Engineering at Texas A&M University in December of 2009. He worked for two years at a construction company until he decided to go back to school to earn his master's degree. He decided to focus on Structures as that was what he was interested in.

Eric currently works at Innovative Engineering Associates as a Structural EIT. He plans to get his PE license and continue learning and gaining experience in the work force.